Engineered nanomaterials and human health: Part 1. Preparation, functionalization and characterization (IUPAC Technical Report)

Vladimir Gubala, Linda Johnston, Ziwei Liu, Harald Krug, Colin Moore, Christopher Ober, Michael Schwenk, Michel Vert

IUPAC Technical Report

Vladimir Gubala*, Linda J. Johnston, Ziwei Liu, Harald Krug, Colin J. Moore, Christopher K. Ober, Michael Schwenk and Michel Vert

Engineered nanomaterials and human health: Part 1. Preparation, functionalization and characterization (IUPAC Technical Report)

https://doi.org/10.1515/pac-2017-0101
Received January 4, 2017; accepted April 19, 2018

Abstract: Nanotechnology is a rapidly evolving field, as evidenced by the large number of publications on the synthesis, characterization, and biological/environmental effects of new nano-sized materials. The unique, size-dependent properties of nanomaterials have been exploited in a diverse range of applications and in many examples of nano-enabled consumer products. In this account we focus on Engineered Nanomaterials (ENM), a class of deliberately designed and constructed nano-sized materials. Due to the large volume of publications, we separated the preparation and characterisation of ENM from applications and toxicity into two interconnected documents. Part 1 summarizes nanomaterial terminology and provides an overview of the best practices for their preparation, surface functionalization, and analytical characterization. Part 2 (this issue, Pure Appl. Chem. 2018; 90(8): 1325–1356) focuses on ENM that are used in products that are expected to come in close contact with consumers. It reviews nanomaterials used in therapeutics, diagnostics, and consumer goods and summarizes current nanotoxicology challenges and the current state of nanomaterial regulation, providing insight on the growing public debate on whether the environmental and social costs of nanotechnology outweigh its potential benefits.

Keywords: analysis; nanomaterial; nanoparticle; nanoscale; nano-toxicology.

CONTENTS

Article note: This document was prepared in the frame of IUPAC Project 2013-007-1-700. Sponsoring bodies: The Chemistry and Human Health Division and the Polymer Division: see more details on p. 1317.

***Corresponding author: Vladimir Gubala,** University of Kent, Medway School of Pharmacy, Central Avenue, Anson Building, Chatham ME44TB, UK, e-mail: V.Gubala@kent.ac.uk. http://orcid.org/0000-0001-6301-3632
Linda J. Johnston: Measurement Science and Standards, National Research Council Canada, Ottawa ONK1A0R6, Canada
Ziwei Liu and Christopher K. Ober: Cornell University, Department of Materials Science and Engineering, 310 Bard Hall, Ithaca, NY 14853-1501, USA
Harald Krug: Empa – Materials Science and Technology, Department of Materials Meet Life, Lerchenfeldstrasse 5, 9014 St., Gallen, Switzerland
Colin J. Moore: FOCAS Research Institute, Dublin Institute of Technology, Kevin St., Dublin 8, Ireland
Michael Schwenk: In den Kreuzäckern 16/1, D 72072 Tuebingen, Germany (formerly Medical School Hannover)
Michel Vert: University Montpellier 1, 15 Avenue Charles Flahault, BP 14491, 34093 Montpellier Cedex 5, France

1 Introduction

Nanotechnology promises to be at the forefront of many 21st century technological breakthroughs. Engineered nanomaterials (ENM) are a class of deliberately designed and prepared materials with nanoscale dimensions that have a rapidly expanding range of applications in our everyday life. The immense interest in nanotechnology and the new opportunities to improve the performance of traditional products that ENM present has led to the development of a 'nano-particle ZOO' [1]. Until recently, many efforts have focused on the use of simple ENM (*e.g.* metal oxides and carbon-based nanomaterials [2]) in applications such as cosmetics [3, 4], energy storage [5, 6], surface coatings [7], and textiles [8]. However, there is now significant interest in more complex nanomaterials, which already have, or are expected to find, an important role as advanced drug delivery systems in nanomedicine, ultra-sensitive reporters in biomedical diagnostics, and multifunctional probes in environmental management and in advanced electronics, transport, information and communication technology, defense, and manufacturing.

The utility of ENM can be attributed to the occurrence of unique size-dependent characteristics that are not exhibited by the bulk material and that lead to useful mechanical, optical, magnetic, and

biological properties. There are many important characteristics to consider, including size distribution, association state, shape, porosity, crystal structure, chemical composition, surface chemistry, charge, stability, degradation, and recycling. Unfortunately, none of these can be singled out as the most important for aspects related to human health. A large number of review articles have summarized the unique structural features and physicochemical properties of nanomaterials that elicit their biological response [9–12].

Nanomaterials are now widely used in commercial products, as illustrated by an article by Vance *et al.* [13] which found that, according to the Nanotechnology Consumer Products Inventory, 1814 nano-enabled products were available in the market (from 622 companies in 32 countries) in the year 2014 (see Fig. 1). Interestingly, 49 % of these products did not declare the composition of the nanomaterial they contained. The majority of nanomaterials used in consumer products were metallic (37 %), with 24 % of products containing silver nanoparticles (NP) (presumably due to their antimicrobial properties). The largest sector (42 %) of the market was attributed to nanomaterials used in Health and Fitness and clearly shows that the impact of nanomaterials on human health will be a key issue for the nanotechnology industry [14].

The objective of this work is to present an overview of ENM with a special focus on those where physical contact with consumers can be expected. Due to the complexity of the topic and the large volume of published material, the account is divided into two separate, albeit interconnected, documents. Part 1 focuses on: i) the preparation of various types of ENM, ii) methods for nanomaterial functionalization, and iii) the analytical tools and methods used for the characterization of their physicochemical properties. Part 2 provides a detailed account of: i) nanomaterials used in therapeutics and diagnostics, ii) nanomaterials in consumer goods, and importantly, iii) the difficulties associated with the study of nanomaterial toxicity. This includes toxicological targets, pharmaco- and toxico-kinetics of nanomaterials, the four nanotoxicology principles, and the current state of nanomaterial regulation.

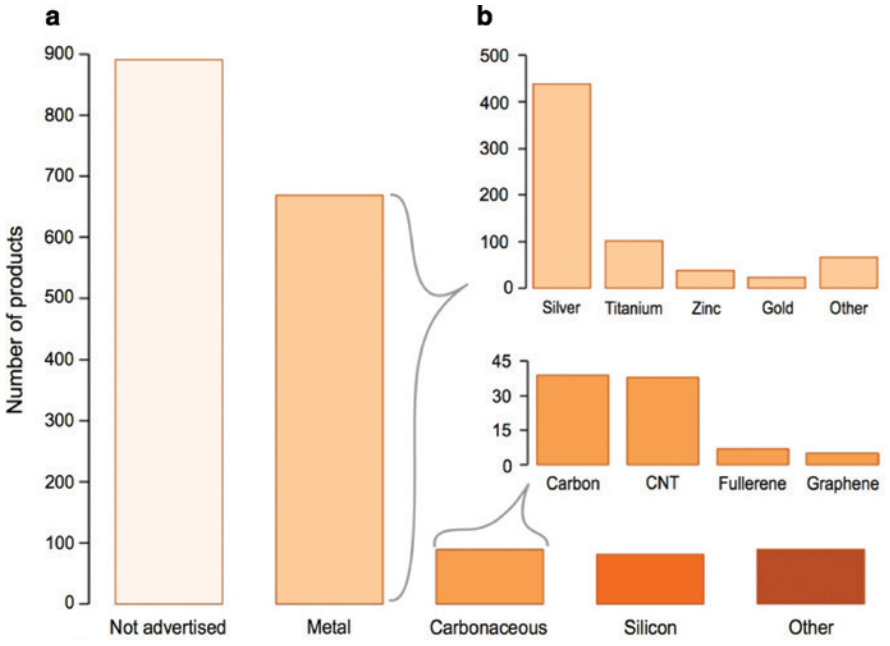

Fig. 1: Nanomaterials in commercially available products in 2014 according to the Nanotechnology Consumer Products Inventory. (a) 49 % of products did not declare the composition of the nanomaterial used. (b) Of those that report the nanomaterial, metallic nanomaterials (particularly silver nanoparticles) were the most heavily used in commercial products (CNT = carbon nanotubes). Reproduced with permission from ref. [13].

2 Terminology for nanomaterials

The broad applicability of nanotechnology has led to considerable variation in the terms and definitions used by various scientific communities and regulatory authorities [15]. Despite this, it is generally accepted that nanomaterials have two defining characteristics: a size on the nanoscale (typically between 1 nm to 100 nm) and unique size-dependent properties that are not exhibited by the bulk material. In an attempt to develop a common approach for describing nanomaterials, a CODATA-VAMAS working group recently released the second version of a Uniform Descriptor System (UDS) for Materials on the Nanoscale [16]. This project aims to develop a system that provides a unique description for nanomaterials and allows one to determine if two materials are equivalent to whatever degree is desired. Nanomaterials cannot be uniquely specified by simple or even complex names, since characteristics such as size, shape, and surface functionality will determine their properties. The UDS is being developed with extensive international consultation, including discussions with the International Organization for Standardization (ISO) and American Society for Testing and Materials technical committees for Nanotechnology, as well as the Organization for Economic Co-operation and Development Working Party on Manufactured Nanomaterials. It is designed to be compatible with the international definition of nanomaterials from ISO technical committee 229 [17] – Nanotechnologies and the European Commission guidelines for regulation of consumer products containing nanomaterials [18]. ISO defines a nanomaterial as a material with any external dimension in the nanoscale or having internal structure or surface structure in the nanoscale; nanoscale is defined as the size range from approximately 1 nm to 100 nm and it is noted that properties that are not extrapolations from a larger size are predominantly exhibited in this size range [19]. Engineered nanomaterials are deliberately designed and prepared materials with nanoscale dimensions, a similar definition to manufactured nanomaterials, which are defined as "intentionally produced nano-sized materials for commercial purposes to have specific properties or compositions". Incidental nanomaterials are generated as an unintentional by-product of a manufacturing, biotechnology, or other process [19].

Both the UDS and ISO TC/229 have adopted "nano-object" as the generic term to describe a material with one, two, or three dimensions on the nanoscale. The UDS has further sub-divided nanomaterials into 4 categories: individual nano-objects, collections of nano-objects, bulk materials that contain nano-objects, and bulk materials with nanoscale features. Although much initial work on nanomaterials focused on approximately spherical particles, there is now significant interest in high aspect ratio particles and one-dimensional materials. A wide range of terms have been used to describe these non-spherical materials. The ISO definition restricts the use of the term nanoparticle to a nano-object with all 3 dimensions on the nanoscale where the lengths of the longest and shortest axes do not differ significantly (see Fig. 2) [20]. This is similar (although not identical) to a definition adopted by IUPAC [21]. The term nanofibre is used for nano-objects with two external dimensions in the nanoscale and the third dimension significantly larger and not necessarily on the nanoscale; the terms nanorod, nanotube, and nanowire are recommended for solid, hollow, and electrically conducting nanofibres, respectively. Finally, the term nano-plate is used for nano-objects with one external dimension in the nanoscale and the other two external dimensions significantly larger. The various terms have not been employed systematically in the literature and a variety of other terms have been used. Where practical, we have adopted the ISO terminology for dealing with nano-objects with one, two, or three dimensions in the nanoscale.

The association of individual nano-objects into clusters is frequently a limitation in preparing suspensions, incorporating nanomaterials in composites, and maintaining their activity in a biological environment. Much of the literature (and ISO definitions) distinguish between the strength of the interactions that lead to the clustering of nano-objects, with the term agglomeration used to describe clusters that are held together by weak forces and that can be disrupted with modest energy input. Aggregates are considered to be clusters of primary particles that are held together by strong forces and are difficult or impossible to disrupt. These terms are generally applied to solid nanomaterials, but are problematic, as there is a continuum of possibilities for the strength of forces leading to the association of individual particles and because the terms are not applied consistently in the literature. There are a number of self-assembled nano-objects (liposomes,

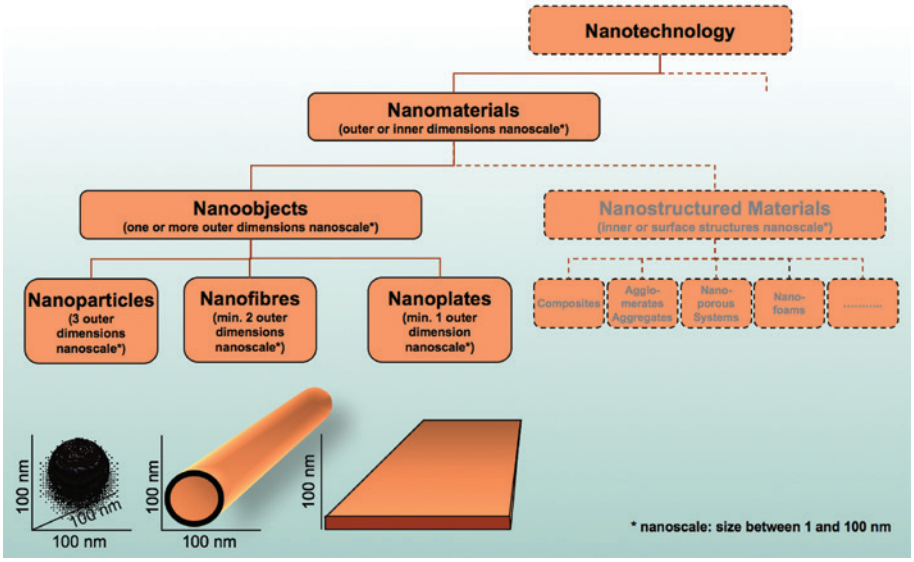

Fig. 2: Classification of nanomaterials. Nanostructured materials (boxes with dashed lines) are not discussed in this review. Adapted from ref. [22].

micelles, mesoporous silica, *etc.*). Some are held together by non-covalent molecular interactions and are particularly important nanomaterials in the context of health and biomedical applications. Self-assembled nano-objects are typically soft materials and frequently have a highly organized structure that is dictated by the intermolecular interactions (π-stacking, hydrogen bonds, hydrophobic, electrostatic, hydrophilic) that lead to their self-assembly (*e.g.* assembly of phospholipid to liposomes). This is in contrast to the clustering or association of solid nano-objects, which is driven by surface interactions. It has been recommended that the terms aggregate and agglomerate be used interchangeably for these soft materials (see IUPAC report [21]). Based on the difference in terminology between various scientific communities, we believe that it may be necessary to distinguish between the association of solid nano-objects and nanosized self-assemblies of molecules. Since in most cases it is not clear which type of association is occurring for specific nano-objects, we avoid the use of aggregation/agglomeration here and instead use the term association.

3 Preparation of engineered nanomaterials

Two general concepts are used to produce nanomaterials: top-down and bottom-up. The top-down method starts with a bulk material from which particles are detached (*e.g.* by ablation or etching) or from which material is erased (*e.g.* lithography). The bottom-up method starts with atoms or molecules that react chemically or are self-assembled to give nanosized particles. The synthetic procedure is followed by a purification step, which usually employs dialysis, chromatography, centrifugation, or ultrafiltration to purify the pristine nanomaterial from the reagents or undesired by-products.

Key quality control factors for the synthesis of ENM include homogeneous composition, narrow size range, stability of the material, and high reproducibility of the method. Engineered nanomaterials with a wide range of compositions, sizes, and shapes are now readily available (see Figs. 1 and 3). Commercial materials include homopolymers, copolymers or biopolymers, self-assembled organic molecules, nanocarbon materials, inorganic oxides such as silica and titanium dioxide, metals, metalloids, quantum dots, and constructs consisting of several of these materials. The various materials are designed to exhibit properties, such as specific band gap energies, superparamagnetism, size-tunable emission, antibacterial activity, textile protection, biocompatibility, and biodegradability. Typically, the size, composition, pore size, and surface

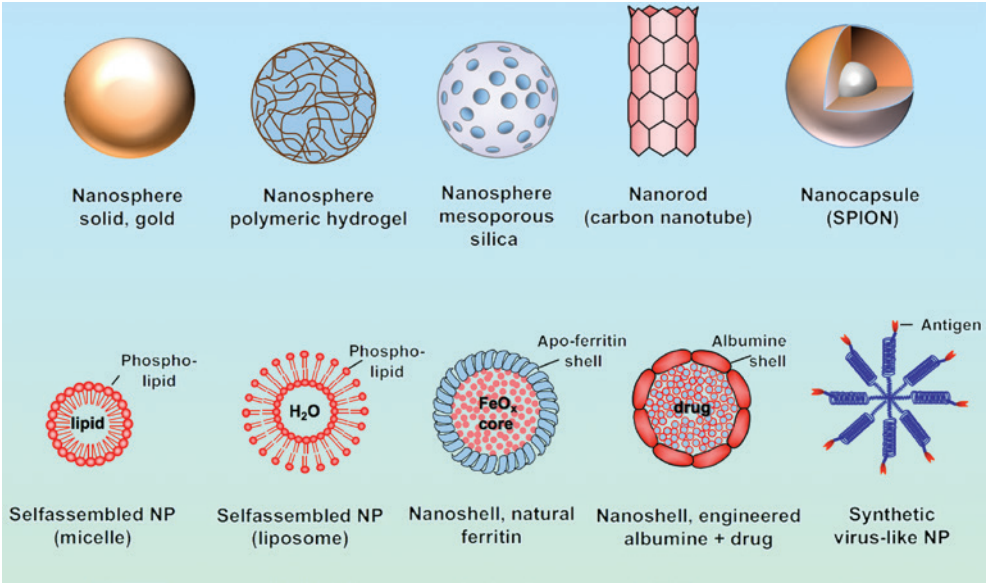

Fig. 3: Schematic illustration of different architectures of Engineered Nanomaterials.

functionalization of the ENM are the main factors that govern its suitability for a particular application. In this section we provide a short overview of the synthetic methods that are used to synthesize common classes of nanomaterials. For each class of material, we also briefly describe the main applications that are likely to have direct impact on the human body and the specific properties that enable them. The application areas include biomedical uses (biosensing and diagnosis, drug delivery, imaging, cancer therapy) and consumer products such as cosmetics, food, and textiles.

3.1 Silica nanoparticles

Silica nanoparticles can be divided into nanoporous (less than 2 nm diameter) and mesoporous (2 to 50 nm diameter) categories depending on their structure. They have significant potential for medical and non-medical applications due to their large surface area, high chemical stability, biocompatibility, and straightforward functionalization. Example applications include filler or reinforcement for advanced composite materials such as dental nanocomposites, food additives (E551: silicium dioxide) in dietary products to reduce the fat content or as anti-caking agents, controls for texture and shelf-life of various cosmetic products, and, recently, new platforms for biomedical applications such as drug delivery and diagnostic testing employed for selecting targeted therapies [23, 24].

Synthetic methods for the production of silica NP include reverse microemulsion, flame synthesis, and sol-gel processing; the sol-gel process is the most widely used, since it provides control of particle size distribution and morphology through the systematic monitoring of reaction parameters [25]. The sol-gel process is based on the hydrolysis and condensation of silicon alkoxides such as tetraethoxysilane (TEOS), commonly known as tetraethyl orthosilicate, in a mixed solution of water and alcohol with either an acid (*e.g.* HCl) or a base (*e.g.* NH_3) as catalyst. In 1968, Stöber developed a reaction system that enabled the controlled growth of spherical silica particles of uniform size ranging from 50 to 2000 nm in diameter [26]. This initial work was followed by the modification of the method to prevent association and produce smaller, homogeneous, and uniformly sized silica NP [27–30]. It has been proven that particle size can be controlled by adjusting reaction parameters, such as solvent, temperature, and concentration of silicon alkoxides and ammonia. Both temperature and concentration affect the rates of hydrolysis and condensation, and hence control the balance between the nucleation and growth processes [27]. The presence of electrolytes in the reaction medium can

also assist in controlling particle size and structure. For example, the addition of small amounts of anionic electrolytes into the reaction mixture produced uniformly sized silica NP with diameters ranging from 20.5 to 34.1 nm, decreasing particle size by more than 70 % [31] when compared to the medium without electrolytes. This occurs because electrostatic repulsion due to anions minimizes particle association and simultaneously inhibits particle growth.

Mesoporous silica NP have been widely explored as drug delivery systems, because their high specific surface area and large pore volume provide unique advantages for the encapsulation of a variety of therapeutic agents [31]. The synthesis is controllable and simple to perform and is based on the formation of liquid-crystalline mesophases of amphiphilic molecules (surfactants) that serve as templates or structure directing agents around which precursors condense to form silica. Various sizes and morphologies with highly ordered mesoporous channels [32] can be obtained by tailoring the molar ratio of silica precursors and surfactants [33], manipulating pH [34], and by adding co-solvent [35]. Ultrasmall sub-10 nm silica particles have been synthesized using hexadecyltrimethylammonium bromide (CTAB) as a structure directing agent and poly(ethylene oxide) (PEO) modified silane to quench particle formation [36]. CTAB acts as a template to generate silica particles with a single pore size and the introduction of PEO generates a modified surface that is suitable for biomedical applications. The same group have since advanced their method of generating ultrasmall silica NP by employing water as a solvent [37].

3.2 Titanium dioxide nanoparticles

Nano-sized titanium dioxide (TiO_2) is used across a wide range of applications, such as paint pigments, glazes, enamels, plastics, paper, fibers, foods, pharmaceuticals, cosmetics, toothpastes, antimicrobial applications, and catalysts for air and water purification or for energy storage [38]. However, nanoscale TiO_2 is predominantly used in personal care products, such as topical sunscreens that block ultraviolet radiation and other skin care products [39]. TiO_2 NP have a greater protective ability than micron sized particles and provide a more transparent product with less residue. Other applications of TiO_2 would also benefit from smaller primary particle sizes. Therefore, the amount of nanoscale TiO_2 used in consumer goods is expected to increase significantly. Food-grade TiO_2 has also been shown to contain up to 35 % primary particles that are less than 100 nm in diameter [40].

The sol-gel method used to make silica NP can also be applied to TiO_2 NP synthesis. The reaction involves the hydrolysis of a titanium precursor, usually titanium alkoxides [41] or titanium halides [42], followed by condensation. Different particle sizes and shapes can be obtained by varying reaction parameters, such as concentration, pH, pore size, and temperature [43]. Surface stabilizers are used to form an insulating organic layer on the surface, preventing particle association. Although sol-gel processes usually result in amorphous materials, different methods have been reported to improve the crystallinity of TiO_2 NP, including calcination [44], ultrasound irradiation [45], and the addition of a base [46], or of salts and acids [47].

Micelles[48] and reverse micelles [49, 50] are also employed for the synthesis of TiO_2 NP. Restricting the reaction to the interior of micelles or reverse micelles provides control of particle size in either aqueous or non-aqueous solution. The ratio of titanium precursor, surfactant, and water; the ammonia concentration; and the reaction temperature are all significant in controlling particle size and size distribution. TiO_2 particles synthesized via this method have an amorphous structure. In order to increase crystallinity while avoiding association, further annealing in the presence of micelles at temperatures considerably lower than those required for the traditional calcination treatment [51] can be applied.

Other popular synthetic approaches include hydrothermal and solvo-thermal methods, which are almost identical except for the use of water and organic solvents, respectively. These methods are normally conducted under high pressure in autoclaves made of steel with PTFE liners, enabling the use of temperatures above the boiling point of a given solvent. Usually, the solvo-thermal method yields better control of size, size distribution, and crystallinity of TiO_2 NP than that achieved with the hydrothermal method, due to the higher boiling point of some organic solvents [44].

3.3 Iron oxide nanoparticles

Iron oxide nanoparticles are the most commonly employed magnetic nanoparticles (MNP). Engineered with a hydrophilic surface coating, they have demonstrated great promise in the biomedical field. Aside from their unique magnetic properties, injectability and high accumulation in the target tissue or organ make them suitable for diagnostic and therapeutic applications, such as magnetic resonance imaging (MRI) contrast agents [52], targeted drug delivery [53], and magnetic field assisted radionuclide therapy [54].

Various methods have been developed to synthesize uniform iron oxide-based MNP with homogeneous composition and narrow size distribution [55]; these include microemulsions [56], sol-gel synthesis [57], sonochemical reaction [58], hydrothermal reaction [59], thermal decomposition [60], and electrospray synthesis [61]. However, the co-precipitation technique is probably the simplest and most efficient method [55]. Fe_3O_4 particles can be synthesized via co-precipitation of iron(II) and iron(III) ions in aqueous solution [62]. Although large amounts of NP can be synthesized in this way, the control of particle size distribution remains a challenge and the nucleation and growth steps must be separated, as explained by LaMer's theory, in order to produce uniform NP [63]. This can be achieved by burst nucleation with hot injection of reagents into the reaction system, which leads to faster nucleation and a concomitant decrease in particle size. Surfactants are necessary to coat the particle surface and prevent the association of smaller particles.

Thermal decomposition is another important method and is now routinely used to prepare iron oxide-based MNP with controlled size and morphology [64]. Metal precursors, usually organometallic complexes, undergo decomposition at high temperature in an organic solvent with surfactant added for NP stabilization and size control. For example, uniform MNP of 20 nm in diameter are synthesized by the decomposition of iron(III) acetylacetonate, $Fe(acac)_3$ at high-temperature (265 °C), in phenyl ether and in the presence of alcohol, with oleic acid and oleylamine as surfactants [65]. FeNP with sizes ranging from 5 to 19 nm can be produced via a similar method by the decomposition of iron(0) pentacarbonyl [$Fe(CO)_5$] in dioctyl ether with oleic acid and oleylamine [66]. Further controlled oxidation transforms them to uniform γ-Fe_2O_3 NP. The size and morphology of NP can be controlled by varying the reaction conditions, including time, temperature, concentration, and ratios of reactants. This method can be extended to alloy particles, such as CoFe and $CoFe_2O_4$, by simultaneous decomposition of $Fe(CO)_5$ and $Co_2(CO)_8$ in 1,2-dichlorobenzene [67], or $Fe(acac)_3$ and $Co(acac)_2$ in hexadecane-1,2-diol [68].

Iron-based MNP can be synthesized through the reduction of metal salts in the presence of surfactant, which prevents particle association [69]. A wide range of common reducing agents, including hydrazine [70], sodium borohydride [71], lithium borohydride [72], and polyols [73], can be used for metal salt reduction. The synthesis of CoFeNP is also achieved by the simultaneous co-reduction of iron(II) sulfate and cobalt chloride salts with sodium borohydride [74]. By using potassium borohydride, hollow CoFe is produced [75]. Reactions carried out in polyols, such as ethylene glycol or propane-1,2-diol, tend to yield more uniform products. Such polyols effectively act as bidentate chelating agents for the solvated metal cations and, in some cases, also serve as reducing and/or stabilizing agents for the metal nanoparticles [76].

3.4 Gold nanoparticles

Gold nanomaterials with novel properties, biocompatibility, and relatively low toxicity, have attracted considerable interest in applications such as diagnostics and therapeutics [77]. More recently, their use in cosmetics and toiletries as anti-wrinkling agents to inhibit the formation of advanced glycation end products has also been explored. Gold nanomaterials can now be divided into two distinct categories: gold nanoparticles (Au NP) and gold nanoclusters. The most interesting property of gold nanoparticles is their tunable surface plasmon resonance, which induces a dramatic enhancement in their absorption and scattering. The surface plasmon band is tunable from the UV to the NIR region by changing the particle size (1 to 100 nm length scale) and shape [78]. Although the term nanoparticle defines an object with all three dimensions below 100 nm, such as spheres, cubes or prisms, the term gold nanoparticle is widely used in

the literature to describe most gold nano-objects, independent of whether they fit this definition (*e.g.* gold rods, plates).

Gold nanoclusters are usually smaller than 3 nm, composed of several to roughly one hundred atoms, and are characterized by the strong quantum confinement effect of free electrons in the particles. Recent synthetic advances enabled the preparation of water-soluble gold nanoclusters with tunable size or emission colors, which accelerated their use as novel labels in biosensing and bioimaging [79].

Significant effort has been devoted to the synthesis of gold nanoparticles, focusing on control over size, shape, solubility, stability, and functionality [80]. Developed by Turkevich *et al.* [81] in 1951, the citrate reduction of $HAuCl_4$ is still one of the most commonly used synthetic methods for Au NP production. In this method, $[AuCl_4]^-$ is reduced by sodium citrate, which acts as both reducing agent and stabilizer, in boiling water. Particles with sizes ranging from 12 to 150 nm can be obtained by varying the nucleation rate and through changing the sodium citrate concentration.

Another breakthrough in gold nanoparticle synthesis is the Brust-Schiffrin method. In this method, $[AuCl_4]^-$ is transferred from an aqueous phase to toluene using tetraoctylammonium bromide as the phase-transfer reagent and reduced with aqueous sodium borohydride in the presence of dodecanethiol. The nanoparticles synthesized are covered with strongly bound thiol-ligands which prevent association. Gold nanoparticles with sizes ranging from 1.5 to 5.2 nm were obtained by adjusting reaction conditions, including the gold to dodecanethiol ratio, temperature, and the reduction rate [82].

A water-based synthetic method is often preferred over the two-phase method, since it uses less toxic solvents and the NP are hydrophilic, and thus more biocompatible. Functional block polymers can also be introduced into the system, where they simultaneously serve as reductants, structure-directing agents, and colloidal stabilizers. For example, in a one-step synthesis of Au NP with an average diameter of about 10 nm, the (PEO-PPO-PEO) block copolymers act as efficient reductants and stabilizers. The reaction takes place in air-saturated aqueous solution at room temperature, and no other reducing agents are needed [83]. When water and commercially available polymers are used, this synthetic method is environmentally benign and economical.

3.5 Silver nanoparticles

Silver has many attractive characteristics that make it applicable to a number of fields, including opto-electronics, catalysis, chemical/biological sensing, *in vivo* imaging, and medicine [84]. Silver nanoparticles (Ag NP) have proven to be particularly attractive as antibacterial agents [85] and are regularly incorporated into apparel to prevent the formation of odour-causing bacteria [86]. They provide an excellent platform for Surface Enhanced Raman Spectroscopy detection and enable single molecule detection. The utility of Ag NP in a variety of applications has led to the investigation of different approaches for nanoparticle preparation using chemical and physical approaches.

Chemical reduction is the most common approach for the production of Ag NP and typically involves three components: (i) metal precursor, (ii) reducing agents, and (iii) stabilizers/capping agents. The most common metallic precursors are silver nitrate, silver acetate, silver citrate, and silver chlorate, while the most frequently used reducers are sodium borohydride and sodium citrate. The main drawback of chemical synthesis is the inability to produce NP of well-defined shape and size. For example, the Creighton method is limited to producing Ag NP of around 10 nm. The Lee-Meisel method, which employs $AgNO_3$ in a variation on the Turkevich method used for Au NP synthesis, produces 30 to 150 nm NP with various morphologies (spheres, polyhedrons, plates) [87]. Reproducible Ag NP synthesis can be related to the initially formed nuclei that can develop into different crystal sizes and morphologies, which are dependent on reaction conditions [88]. Indeed, it has been highlighted that even small impurities in silver nitrate can influence the shape and crystal structure of the resultant NP, as reviewed by Xia [89]. The association of Ag NP is typically prevented through the introduction of stabilizing agents, such as poly(N-vinylpyrrolidone), on the particle surface. Bastuś *et al.* reported the controlled synthesis of highly uniform citrate-stabilized Ag NP by reducing $AgNO_3$

using a combination of sodium citrate and tannic acid [87]. Small, uniform Ag NP (10 to 20 nm) could be produced by varying the molar ratio of tannic acid to sodium citrate (0.005:1 up to 1:1). Particles of defined size (*e.g.* 15 nm) were then used as 'seeds' for the subsequent production of larger uniform NP by sequentially adding more sodium citrate, tannic and $AgNO_3$ in a defined ratio. The new generation of well-defined larger NP was then used as new 'seeds' to create even larger NP with a narrow size distribution. Overall, the authors reported the ability to produce citrate-stabilized Ag NP over a range of 10 to 200 nm with standard deviation less than 10 %.

Prominent physical methods of Ag NP production are laser ablation and evaporation/condensation. Laser ablation involves the use of a silver plate immersed in a liquid phase. A focused, high-energy laser irradiates the metal to generate a heated plasma containing a high concentration of silver atoms and ions that cool in the solvent, facilitating Ag NP growth [90, 91]. A number of factors govern the size, shape, growth rate, and uniformity of the resultant NP. These factors include the laser wavelength, pulse duration (femto-, pico- or nanosecond regime), laser fluence, ablation time, and the solvent properties [92]. Another physical preparative method is the evaporation/condensation technique, which uses a tube furnace. One advantage of physical synthesis methods is that they do not require chemical reagents and can therefore generate high purity colloids.

Alternative 'green synthesis' methods of generating Ag NP are becoming increasingly popular. Green synthesis uses biological sources, such as bacteria [93], fungi [94] and plants [95], which have naturally occurring biocompatible reducing agents and stabilizers for NP generation. These methods circumvent the need to use potentially harsh chemical agents and aim to minimize the environmental impact of NP production. However, the scalability of such approaches remains unresolved. A recent example of this was demonstrated by Giessen and Silver when they engineered 25 nm diameter encapsulins from *Thermotoga maritima* to produce 13.5 nm Ag NP. Encapsulins are a new class of microbial nanocompartments and were exploited to confine particle growth [93]. This was enabled by genetically modifying the encapsulin to display the silver-binding AG4 peptide, first reported by Naik *et al.* [96], on their compartmental interior. The authors highlighted that the exact mechanism of silver precipitation by AG4 remains to be fully elucidated. However, the hydroxyl groups of tyrosine residues have been shown to be active in silver ion reduction [97] and NMR studies of |AG4 by Lee *et al.* [98] reported shifts in the hydrophobic side chains of leucine, phenylanaline, and arginine during Ag NP formation, indicating that they may serve as NP formation sites.

3.6 Quantum dots (QD)

Quantum dots (QD) are nanoscale semiconductor crystals that are generally composed of elements from groups 2–4, 3–5, or 4–6 and have sizes ranging from 2 to 10 nm [99, 100]. They have size dependent optical properties that are due to quantum confinement effects on electronic states. QD have unique advantages over traditional fluorescent dyes, including a broad excitation range, narrow and size-tunable emission, high luminescence yields, and good photochemical stability [101], making them appealing *in vivo* and *in vitro* fluorophores in biological applications [102].

Since Brus *et al.* first reported colloidal QD in 1983 [103], researchers have been developing synthetic methods for these nanomaterials. The current methods can be divided into two classes: organometallic synthesis based on high-temperature thermolysis and aqueous synthesis with thiols as stabilizers [100]. In 1993, Bawendi *et al.* reported a simple route for the synthesis of high-quality near-uniform 2–6 QD by injecting organometallic reagents, such as dimethylcadmium, into hot coordinating solvent, which provided temporally discrete nucleation, as well as the controlled growth of macroscopic quantities of QD with sizes from about 1.2 nm to about 11.5 nm [104]. This method was later optimized to a one-pot synthesis by using cadmium oxide as the precursor instead of dimethylcadmium, which is difficult to handle and unstable [105]. Core-shell QD, in which the higher-band-gap shell protects the inner core from oxidation and improves the photoluminescence quantum yields, provides materials with novel properties that are more attractive for applications [106]. Examples of core-shell QD include CdS/CdSe [107], CdS/ZnS [108], and CdSe/ZnS [106, 109]. In the synthesis

of CdSe/ZnS QD, uniform CdSe quantum dots are first synthesized through pyrolysis of Cd and Se precursors and then injected into a solution of trioctylphosphine oxide to which Zn and S precursors are added dropwise under a N_2 atmosphere to form a ZnS layer. When prepared in organic solvent, the poor aqueous dispersibility resulting from hydrophobic surface ligands makes QD unsuitable for biomedical applications. Therefore, ligand exchange with hydrophilic molecules and polymers or silica coatings is necessary, as discussed below.

Compared to thermolysis in organic solvents, aqueous methods are preferable, since they are cheaper and more reproducible, use less toxic materials, and produce biocompatible QD with high aqueous stability and biocompatibility [110]. This makes them more promising for biomedical use [111], even though they have lower photoluminescence quantum yields and therefore significant effort has been directed towards aqueous synthesis methods [110]. In the synthesis of CdTe, cadmium perchlorate is dissolved in water in the presence of NaHTe followed by addition of a thiol stabilizer such as 2-sulfanylethanol [112], 2-sulfanylacetic acid [113] or cysteine [114], which are soluble or miscible in water at appropriate pH. CdTe nanocrystals with excellent aqueous dispersibility are produced after refluxing under aerated conditions [115]. By taking advantage of high temperature hydrothermal synthesis techniques, the photoluminescence quantum yield and size distribution of CdTe QD are significantly improved [110]. In order to modify this time-consuming procedure, microwave radiation is often introduced [116]. Studies have shown that microwave assisted aqueous synthesis is generally faster, simpler, and more energy efficient compared to conventional hydrothermal synthesis [117, 118]. It is believed that fast and uniform heating from microwave radiation results in good crystallinity and high quality QD.

3.7 Polymeric nanoparticles

Polymeric materials have been used in a range of pharmaceutical and biotechnology products for more than 70 years. Polymer-based multifunctional nanoparticles capable of targeting, diagnosis, and drug delivery were developed more recently [119]. Polymeric NP can be loaded or coated with drugs and can be used to administer, carry, and deliver drugs [120]. Ever since Langer and Folkman reported sustained release of biochemically active macromolecules from biodegradable polymers in 1976 [121], polymer-based NP have impacted virtually every branch of medicine [122]. Today, the most commonly used polymers for drug release applications include poly(D,L-lactic acid)-*co*-(glycolic acid) (PLAGA), poly(lactic acid) (PLA) and poly(glutamic acid) (PGA), due to their favorable bioavailability, biocompatibility, biodegradability, and low toxicity [123]. Some polymer-based NP have received regulatory approval as drug delivery systems in humans [124, 125].

A number of bottom-up and top-down methods are available for the preparation of polymeric NP. The bottom-up techniques – emulsion, interfacial and precipitation polymerization – employ a monomer as the starting point [126]. The top-down techniques include solvent emulsion evaporation [127–130], solvent displacement [131, 132], and salting out methods [133, 134] and start with a polymer that is preferably bio-resorbable and ideally bio-degradable *in vivo* [135]. The presence of surfactant is essential to prevent nanoparticle association and ensure the stability of nanodispersions. Solvent emulsion evaporation is the most common technique and requires the emulsification of the polymer solution as the first step, followed by homogenization of the resulting mixture [136]. The emulsification method can be divided into two categories, oil-in-water (O/W) emulsification (single emulsion), and water-in-oil-in-water emulsification, W/O/W (double emulsion). The O/W emulsification technique is suitable for entrapping hydrophobic drugs, while W/O/W is generally used for the encapsulation of hydrophilic drugs and proteins [128, 137]. The size of polymeric NP can be controlled by adjusting reaction parameters, such as stirring rate, temperature, and the type and concentration of dispersing agent [138].

Solvent displacement, also called nanoprecipitation [132], involves the use of an organic solvent that is miscible with an aqueous phase in the presence or absence of surfactant [131, 139–141]. Polymers and drugs are dissolved in the organic solvent and are transferred to an aqueous solution, where the hydrophobic polymers

and drug self-assemble into core-shell nanospheres that precipitate [142]. This technique is amenable to scale-up to an industrial scale and requires only gentle stirring with no high shear stress [126].

Non-degradable polymers, such as polystyrene, also play an important role in this field. In medicine, polystyrene microspheres have been used in the treatment of hepatocellular carcinoma, based on the principle that the vascular bed of many solid tumors is hyperpermeable to macromolecules and nanoparticles, allowing their accumulation in tumors [143]. The synthesis of polystyrene particles is typically accomplished by bottom-up polymerization, although this method cannot independently control particle size and molecular weight [144]. Top-down techniques such as nanoprecipitation were also employed [145, 146].

"Intelligent" nanoparticles composed of stimulus-responsive polymers, for example pH-responsive polymers (*e.g.* poly(acrylic acid)) and thermal-responsive polymers (*e.g.* poly(*N*-isopropylacrylamide)), have been extensively studied. When subjected to external signals they produce physical or chemical changes that include variations of macromolecular structures, solubility, surface properties, swelling, and dissociation [147]. Most stimulus responsive polymers are synthesized via bottom-up techniques. Conjugated polymers also show potential for biomedical applications. For example, cyanovinylene–backbone conjugated polymers can be used as *in vivo* nanoprobes due to their high chromophore density and high fluorescence efficiency [148]. The nanoparticle synthesis method is quite similar. In this case, hydrophobic monomers are dissolved in a neat liquid surfactant and then micellized in water, allowing polymerization to occur in the nanoscopic non-polar interior of the micelles.

3.8 Carbon nanotubes

Carbon nanotubes (CNT) are hollow nanofibers (see Fig. 2) whose walls are composed of sheets of graphene that exhibit a hexagonal arrangement of sp^2-hybridized carbon atoms and were first observed and described by Radushkevich and Lukyanovich in 1952 [149]. Their unique structures result in impressive mechanical, thermal, magnetic, optical, electrical, surface, and chemical properties that have potential for extensive biomedical applications in areas such as *in vivo* imaging, biosensing, and drug delivery [150, 151]. CNT are divided into two basic forms, single walled carbon nanotubes (SWCNT) consisting of a single tube of graphene, and multiwalled carbon nanotubes (MWCNT) composed of several concentric tubes of graphene.

Arc discharge, laser ablation, and chemical vapor deposition are the three main production methods for CNT. The simplest method to achieve large-scale synthesis applies a DC arc discharge between two graphite electrodes in the presence of a metal catalyst at low pressure in a controlled atmosphere composed of inert/or reactant gas [152]. The catalyst used and the type and pressure of the gas affect the CNT morphology, purity, and yield. Researchers concluded that arc discharge in an organic atmosphere produced more MWCNT because organics could be ionized and decomposed into hydrogen and carbon atoms, which contribute to MWCNT synthesis.

Laser ablation, another synthetic method for CNT first demonstrated in 1995 [153], favors the growth of SWCNT with controlled diameter depending on reaction temperature. The principles and mechanisms are similar to arc discharge with the difference that the energy is provided by a laser beam focused onto a metal-graphite composite target, which is placed in a high-temperature furnace. A number of factors including laser intensity, furnace temperature and metal catalyst affect the size, morphology, yield, and physical characteristics of SWCNT [154].

Chemical vapor deposition is now the standard method for synthesis of CNT. It is not only controllable, but also economically viable for large scale CNT production [155]. This method involves decomposition of various hydrocarbons over a transition metal supported catalyst, which can be carried out at atmospheric pressure [152] in a temperature range of 300 to 1200 °C [156]. A variety of gaseous and liquid hydrocarbon feedstocks can be used as precursors. Besides transition metals and rare earth elements, catalysts formed from metals combined with natural minerals, such as forsterite, diopside, quartz, and magnesite, have also been used [157].

3.9 Liposomes

Although liposomes are not typically considered to be a class of ENM, they are often functionalized to have novel properties for biomedical applications. Liposomes have significant potential for drug delivery and currently represent the majority of the clinically approved nano-enabled therapeutics. Drug delivery applications typically require the functionalization of the liposomes to improve stability and incorporate targeting moieties. Liposomes came to prominence in 1965 following work by Bangham [158] in which the amphiphilic nature of their structure was revealed through the identification of the phospholipid bilayer. They are used to carry hydrophilic drugs in their interior and hydrophobic drugs inside the membrane, which has led to liposomes becoming the most widely studied drug delivery nanomaterial for cancer treatment.

Several techniques, such as Bangham's method, detergent-depletion, reverse phase evaporation, ether/ethanol injection and emulsion methods, as well as alternative methods including dense gas and supercritical fluid techniques have been reported and reviewed elsewhere [159, 160]. Due to the differences in preparation methods and lipid compositions, liposomes can be classified according to their lamellarity (uni- and multilamellar vesicles), size (small [diameter below 100 nm], intermediate [100 to 250 nm], or large [above 250 nm]), and surface charge (anionic, cationic, or neutral). The 'First generation' liposomes used for drug delivery suffered from problems, such as rapid accumulation in mononuclear phagocyte system organs (*e.g.* liver and spleen). Their circulation half-life has been dramatically improved by grafting biocompatible polymers, such as polyethylene oxide, to the liposome surface. This class of liposome has since been dubbed 'stealth liposomes' [161]. In the case of the commercially available stealth liposome Doxil®, a liposome platform encapsulating the chemotherapy drug doxorubicin, a circulation half-life 100 times that of free doxorubicin is observed [162]. Doxil® has also been shown to lower cardiotoxicity 7-fold in comparison to free doxorubicin. Liposomes are widely available commercially, with global sales in the hundreds of millions of dollars annually. Doxil® and Myocet® encapsulate the chemotherapy drug doxorubicin, with the latter being a non-PEGylated liposomal system. AmBisome® is a liposomal formulation of the broad-spectrum polyene antifungal agent amphotericin B [163].

3.10 Bioinspired nanomaterials

Biomacromolecules are typically nanosized, more or less bio-tolerable, and intrinsically biodegradable, provided suitable enzymes are present and the macromolecules have not been chemically modified. These properties make them attractive starting points for producing engineered nanomaterials for biomedical applications. Proteins, such as serum albumin and ferritin, and nucleic acids are among the more commonly used biomacromolecules in NP synthesis. Serum albumin, the predominant protein in blood, has binding sites for amphiphilic molecules and can be cross-linked, for example using glutaraldehyde, to form nanoparticles. Cross-linking in the presence of a drug generates a nanoparticle that can be used for slow drug release [164]. However, excessive use of glutaraldehyde as the cross-linker can inhibit the degradability of the nanomaterial and, as the particle degrades, the released glutaraldehyde may cause undesirable interactions with other molecules in the body. Ferritin is an 8-nm diameter iron-storage protein that consists of 24 identical subunits that form a cavity containing approximately 4000 iron(III) atoms. The high iron content makes ferritin a useful contrast agent for imaging techniques [165]. In addition, disassembly of the protein scaffold provides a source of iron nanoparticles and its reassembly in the presence of a drug provides a novel drug delivery system. In a third example, viral structural proteins can self-assemble *in vitro* to give virus-like particles that lack genetic material. Incorporation of antigens provides a powerful vaccine and virus-like particles can also be used to encapsulate drugs [166]. Similarly, encapsulins, which are spherical bacterial organelles with a diameter of about 30 nm, have been used to engineer nanosized materials.

DNA nanostructures can be engineered by programmable self-assembly to give well-defined architectures (DNA origami). These nanostructures can be equipped with functional groups at preselected sites and are promising substrates for vaccination, drug delivery, and other applications [167]. Similarly, RNA

nanoparticles can be assembled from suitable precursor RNA strands [168]. When engineered from RNA strands that influence gene-expression (interference RNA) or carry catalytic activity (catalytic NA), they are a promising approach for various biotechnology applications. Moreover, carbohydrates of various chain length and composition (*e.g.* dextran, chitosan) have been used either with or without further modification as the basis for ENM. Carbohydrate-based nanoparticles have been highlighted for their medical applications for diagnostics and therapy, molecular imaging, and drug delivery, particularly in cancer chemotherapy.

4 Surface functionalization of nanomaterials

Most nanomaterials require modification or functionalization, either during the initial synthesis or for post-synthesis applications (see Fig. 4). In some cases, modifications are necessary to improve the stability of the nanomaterial (towards dissolution or association), to change its hydrophobicity or hydrophilicity for dispersion in appropriate solvents, or to enhance biocompatibility. In other cases, surface functionalization may protect or improve the performance of the core material or reduce the overall cost of the material. Water-soluble functional nanomaterials are indispensable for various biomedical applications, but most of the good synthetic methods for noble metals, quantum dots, and magnetic metal oxides produce nanomaterials with a hydrophobic surface [78]. Therefore, water solubilization and functionalization to convert hydrophobic NP into hydrophilic ones and the introduction of additional chemical functionality are key steps for applications [169]. Different strategies have been used to functionalize nanoparticles with a variety of ligands, such as small molecules, surfactants, polymers, and biomolecules [170]. For therapeutic applications, it is common to introduce a polymer coating that is biocompatible (for example PEO, known by its trivial name PEG) and also to include targeting moieties. These include a variety of bio-recognition elements, such as antibodies, nucleic acids, peptides, and ligands for specific receptors. In many cases, the functionalization of the nanomaterial can be used to produce a multifunctional platform that incorporates both drug delivery and diagnostic imaging capabilities. The procedures used for surface modification and stabilization include many chemicals, some of which can have a significant effect on NP properties. Precise information is required on the qualitative and quantitative presence of the ligands and stabilizing moieties attached to the surface,

Function of modification	Coating material	Comments	Figure
Increase of suspension stability	Molecules, polymers (10 – 100 kDa), charged polymers (electrolytes, surfactants)	One layer, mostly applied during production or during processing	
Improvement of wettability	Molecules, polymers, inorganic layers	For an easier production of nanoparticles mixtures with water (hydrophilic) or organic solvents and polymers (hydrophobic)	
Decreased solubility	Inorganic layers, mostly silica	Smaller particles have an increased solubility. Layer shall retain the chemical properties (ZnO/SiO_2; Ag, Au/SiO_2)	
Improvement of physical and chemical function, improved efficiency	Inorganic layers, mostly silica or ZnO in combination with SiO_2	Strong increase in fluorescence of quantum dots, if free surface bonds are saturated	
Reduction of costs and material	Noble metals e.g. palladium	Thin, incomplete layers of noble metal as a catalyst on cheap carrier material	
Protection	Organic layers	Protection of particle functionality e.g. from catalyst poisoning	
Biocompatibility and functionality	Biocompatible polymers and inorganic layers, antibodies and peptides	Biocompatible SiO_2 or polyethylene glycol (PEG) can decrease corona effect. Antibodies used for targeting cells.	

Fig. 4: Surface-modifications of ENM. Adapted from 'Coatings for nanomaterials', ref [171].

as well as residual reagents that may not have been removed during purification. In the case of targeting ligands, it is particularly important to control their surface orientation and verify that they retain their native binding affinity for the receptor of interest.

Here we review five of the most common strategies for nanomaterial functionalization: silica coating, ligand exchange, polymer coating, surface modification of carbon nanotubes, and bioconjugation to introduce targeting moieties. The general challenges and approaches used for surface modification and functionalization are summarized in several recent reviews [172–179].

4.1 Silica coatings

The introduction of a silica coating is one of the most widely used methods for the surface functionalization of NP [180, 181]. Silica serves as a robust layer that prevents the degradation of optical properties, imparts water solubility, and protects the core NP from the external environment [182, 183]. Classic silica coating methods include the use of silane coupling agents [184], the Stöber method [185, 186], and reverse microemulsion [187]. Silica coatings can be grafted on most types of nanomaterials that have a chemical or electrostatic affinity for silica. Silica coating is usually formed as a one to tens of nanometer-thick porous silica shell on the surface of the nanomaterial core [188]. This process is frequently referred to as silanization in the literature [189–191].

The concept of silane coupling agents was reported by Plueddemann and his coworkers in 1962 [184]. Since then researchers have developed silane coupling agents with different functional groups for NP surface modification. As examples, (3-methacryloxy)propyl]trimethoxysilane [192], (3-aminopropy)ltriethoxysilane (APTES) [193], (3-isocyanatopropy)ltrimethoxysilane [194] and 3-(trimethoxysilyl)propyl methacrylate [195] have been used to functionalize nanoparticles with surface hydroxyl groups, such as silica, TiO_2, and Fe_3O_4 NP. The methoxy/ethoxy groups of these silanes condense on the NP surface, forming a silica layer around the particle. As a result, functional groups are imparted on to the NP surface and are available for future reactions.

A very common approach for the preparation of silica shells is the Stöber method, in which as-prepared NP act as seeds for silica growth in an ethanol/water mixture and yield core-shell spheres. The prerequisite for this method is that the NP surface must have a significant chemical or electrostatic affinity for silica. Silanes can directly polymerize on oxide NP, such as Fe_3O_4 and TiO_2, that have hydroxide-terminated surfaces; silane hydrolysis and condensation take place under basic conditions. However, for NP that do not have a passivating oxide layer in solution, such as noble metal and quantum dots, a ligand exchange using 3-(trimethoxysilyl)propyl methacrylate and APTES [196] is necessary to render the particles hydrophilic before the Stöber method is applied to grow thicker silica shells. The ligand exchange mechanism will be discussed in the next section. In 2003, Graf *et al.* developed a simpler and faster method based on the use of poly(vinylpyrrolidone) (PVP), which has been shown to adsorb onto a wide variety of colloidal particles [197, 198]. Upon PVP adsorption, the particles are transferred into a solution of ammonia in ethanol and directly coated with a silica layer of variable thickness by the addition of TEOS in a seeded growth process [197]. The particle stability and homogeneity of the coating shell are significantly affected by the molecular weight of PVP. Longer PVP chains improve the stability of the particles but lead to a rough surface coating. Thus, the optimal PVP lengths for coating different-sized NP usually have to be determined empirically.

The reverse microemulsion method is an alternative approach for silica shell formation. This method provides nanoreactors for the confined synthesis and silica coating of nanoparticles [187]. It can be applied to both hydrophilic QD stabilized with 3-sulfanlpropanoic acid or sulfanylacetic acid and hydrophobic QD prepared by the trioctylphosphine/trioctylphosphine oxide method [199]. In a reverse microemulsion, small water droplets are stabilized by a surfactant in a hydrophobic continuous phase. Hydrolysis and condensation of the silica precursor (*e.g.* TEOS) take place at the water-oil interface or in the water phase, resulting in highly uniform silica particles [200]. Hydrophilic QD coated with 3-sulfanylpropanoic acid or 2-sulfanylacetic acid transfer easily into the small water droplets, where silica growth occurs. For hydrophobic QD, hydrolyzed

TEOS molecules replace the original hydrophobic ligands, facilitating the transfer of the QD into the hydrophilic interior of the micelles. The reverse microemulsion method has better control over particle size and size distribution than the Stöber method [201].

4.2 Ligand exchange

The use of small ligands that can replace the initial as-synthesized surface coating is a popular strategy for NP surface modification [202]. Highly crystalline and uniform NP are prepared in organic solvents at high temperatures using a stabilizer-modified surface that controls growth and prevents association during synthesis. This normally yields hydrophobic NP; ligand exchange is then used to render the NP hydrophilic and suitable for biomedical applications [203].

Ligand molecules usually have two parts: the anchoring groups and the functional groups. The former bind the ligand onto the NP surface with high affinity, while the latter provide colloidal stability and functionality for further applications [202]. The choice of ligand depends on the core materials, particle size, and the solvent used. For example, QD and noble metal NP have surfaces that can easily bind thiols, disulfides, phosphines, and amines [102]. Metal oxide NP surfaces typically bind phosphonic acids and carboxylic acids [204].

Trioctylphosphine/trioctylphosphine oxide-coated quantum dots are usually transferred to aqueous solution by replacing the original hydrophobic ligands with hydrophilic thiol-based ligands, such as 2-sulfanylacetic acid, 3-sulfanylpropanoic acid, 11-sulfanylundecanoic acid, or 2-sulfanylsuccinic acid. Bidentate and multidentate molecules (for example, 6,8-disulfanyloctanoic acid [205, 206], and carbodithioate ligands [207]) have also been developed, as they are more strongly anchored to the NP surface and provide longer-term colloidal stability than monodentate ligands. The carboxylic acid groups on these ligands also increase NP colloidal stability by charge repulsion and have flexible conjugation sites [208]. At the appropriate pH, other charged ligands with quaternary amine, tertiary amine, or sulfonic acid groups can also endow NP with excellent colloidal stability [209].

A second strategy for ligand modification is surfactant addition, during which the hydrophobic moiety of the surfactant associates with the hydrocarbon chain of the initial surface ligands, while the hydrophilic groups are exposed on the surface of the NP, rendering them water soluble [64]. CTAB is a widely-used surfactant and a known phase transfer agent. When dodecylamine-capped gold nanoparticles in chloroform are mixed with water containing CTAB, the hydrocarbon chain of CTAB assembles on the dodecylamine layer by hydrophobic interaction and the positively charged ammonium moieties extend into the solution, resulting in transfer of the hydrophobic nanoparticles into the aqueous phase [210].

4.3 Polymer coating

ENM that are designed for biomedical applications may be recognized as foreign objects and therefore eliminated from the blood stream by the reticuloendothelial system [211, 212]. To avoid premature ENM clearance by the immune system and prolong their half-life in circulation, it is common to introduce “stealth” properties [213] by surface modification with biocompatible polymers [214, 215]. The preferred method is the adsorption or grafting of poly(ethylene oxide) (PEO), a linear polymer consisting of repeat units of $-CH_2-CH_2-O-$. A version of this polymer, terminated on both ends with –OH groups, is very well known as poly(ethylene glycol) (PEG). The two terms are used in the literature interchangeably. The systematic term PEO is used more in chemical and polymer sciences, while the trivial term PEG is very common in biological and material sciences. In fact, the popularity of the trivial term PEG gave rise to the word ‘PEGylation’ and its analogues to describe the process of attaching segments of PEO to virtually any object or molecule. The term PEGylation is now extensively used across many scientific disciplines (including polymer science) and is also used in this document. We will however, refrain from using PEG, replacing it with the IUPAC-recommended, systematic term PEO.

PEGylation of NP can be accomplished by covalently grafting, entrapping, or physically adsorbing PEO segments to the NP surface [216–219]. There are two synthetic approaches: a one-pot method where *in situ* formation of NP and polymer coating take place concurrently, and a two-step method where the NP are first prepared and then coated with polymer [212]. Physisorption of PEO onto gold NP surfaces can be achieved through the one-pot method. An aqueous mixture of gold precursor and PEO is bombarded with synchrotron X-rays and PEO-gold NP are formed [220]. Covalent bonding is more complicated, since a thiol-functionalized PEO is used to passivate the gold surface with thiol groups and form a poly(ethylene oxide) layer on the NP surface. Both the PEO molecular weight and the type of anchoring ligand affect the stability of the PEO-coated NP [221]. Gold NP coated with high-molecular-weight PEO are more stable than those with low-molecular-weight PEO, while NP coated with thioctic acid-anchored PEO exhibit higher colloidal stability than NP coated with thiol-anchored PEO [222]. The PEO coating can be further functionalized with additional moieties, such as antibodies, proteins, dextran, and DNA.

PEGylation of metal oxide NP usually involves introducing a silane between the surface and the PEO layer. This approach can be achieved either by reacting the NP with silanes and then functionalizing with PEO, or by reacting NP with commercially available PEO-siloxane. In the latter case, oleic acid-capped Fe_3O_4 NP undergo a ligand exchange reaction with PEO-siloxane in toluene, and the PEO coated NP are soluble and stable in aqueous solution [223]. One-pot PEGylation of metal oxide NP is usually achieved in one of two ways: co-precipitation of salts or thermal decomposition of metallorganics in the presence of polymer. In the case of co-precipitation, PEO-coated Fe_3O_4 NP with various sizes have been synthesized by treating iron(II) and iron(III) solution with a base in the presence of PEO-containing graft copolymer, poly(glycerol monoacrylate)-g-poly(PEO methyl ether acrylate). The polymer block is chemisorbed to the particle surface by the coordination of 1,2-diols to the Fe atoms while the PEO block extends into the water [224]. Similarly, PEO-gallol can be coated onto Fe_3O_4 NP. The high binding affinity of the gallol and trihydroxybenzene units toward iron oxide allow a successful re-dispersion of freeze-dried particles [225]. Another one-pot synthesis of Fe_3O_4 NP functionalized with monocarboxyl-terminated PEO is achieved by the thermal decomposition of ferric triacetylacetonate ($Fe(acac)_3$) in the presence of carboxy-PEO via coordination between carboxylic acid and Fe on the NP surface. Particle size is determined by the molecular weight of carboxy-PEO and the concentration of $Fe(acac)_3$, as well as by the ratio between them [226].

Block polymers are even more powerful NP stabilizers than homopolymers because they undergo phase separation and exhibit unique properties, such as surface reactivity, elasticity, selectivity, and resistance [227]. For example, degradable PLAGA NP can be coated with an amphiphilic PEO-PLA diblock copolymer, in which the hydrophobic PLA block adsorbs on the PLAGA surface and the hydrophilic PEG block extends from the NP surface and forms a protective coating [228]. However, such physically adsorbed polymers may not be stable and may undergo desorption *in vivo* due to replacement by blood components with higher affinity to the NP surface. Therefore, covalent binding of polymer is preferred in order to increase coating stability. A series of amphiphilic di-block copolymers of biodegradable PLAGA or PLA with PEO has been produced through ring opening polymerization of monomers in the presence of monomethoxy PEO [229]. Different solubility of the two blocks results in phase separation and a core-shell structure can be formed by an O/W emulsification procedure [230]. Although it is generally accepted that PEO-based coatings repel proteins, some poly(ethylene oxides) seem to be compatible with proteins. For example, a surface modified with PLA-PEO was reported to be able to adsorb proteins [231], provided that these proteins were present at their physiological concentrations [232].

4.4 Surface coatings of carbon nanotubes

Despite the promising biomedical applications of CNT, the high cytotoxicity attributed to their highly hydrophobic surface and their lack of biodegradability [233] limits their use in many biological systems. Therefore, surface modification and functionalization of CNT to improve their solubility and biocompatibility has become a prerequisite for their applications. Many studies have shown that increased solubility of functionalized CNT improves their performance and lowers their toxicity [234, 235], as they have low association and

can be taken up into cells without decreasing cell viability [236]. Functionalization strategies fall into two categories: covalent and noncovalent functionalization.

Covalent functionalization is based on the covalent linkage of functional entities onto the nanotube's carbon scaffold [237]. The reaction occurs with a change of hybridization of the carbon atoms from sp^2 to sp^3 with concomitant disruption of extended π-conjugation, leading to the introduction of defects in the nanotube structure with consequences for electron-acceptor and/or electron transport properties [238]. Oxidative purification is one of the most common functionalization techniques and can be achieved by using nitric acid [239–241], sulfuric acid [242], piranha solution [243], or gaseous dioxygen [244, 245] as an oxidant. Through this method oxygen-bearing functionalities, such as hydroxy, carbonyl, and carboxylate groups, can be introduced to CNT, while residual metallic catalyst and carbonaceous impurities can be removed [246].

Noncovalent functionalization is achieved through weak interactions (π-π stacking, electrostatic interactions, hydrogen bonding, and van der Waals forces) between molecules and CNT sidewalls. This helps to increase the water miscibility of CNT and leaves the polyaromatic scaffold unperturbed. The sp^2 nanotube structure of CNT and their electronic characteristics are preserved [247]. Generally, small aromatic molecules are the ideal candidates to bind to CNT sidewalls and function as sites for further derivatization [248]. Proteins are shown to be able to bind to CNT surfaces via a covalent sidewall functionalization. As such, a variety of proteins have been successfully immobilized on SWCNT functionalized by 1-pyrenebutanoic acid succinimidyl ester, in which the pyrene moiety adsorbs onto the sidewalls of SWCNT via π-π interactions [249].

Adsorption of surfactants onto a CNT surface is another widely used method that can enhance the stability and dispersibility of CNT. Self-assembly of surfactants on the CNT sidewalls changes the surface from hydrophobic to hydrophilic and therefore reduces the CNT cytotoxicity [250]. Surfactants such as sodium dodecyl sulfate, lithium dodecyl sulfate, CTAB, and Triton-X have been shown to disperse CNT effectively [151]. Finally, coating CNT with functionalized polymers is a common strategy to impart biocompatibility and solubility of the nanomaterial. For example, in the case of fluorescein-polyethylene glycol, the hydrophobic aromatic fluorescein group binds to the sidewall of SWCNT (likely via π-π stacking), while the PEO group extends into the water [251]. Other polymers, such as poly(vinyl pyrrolidone) [243, 252], poly(vinyl alcohol) [253], and poly(ethylene oxide) [254], have also been reported to modify CNT surfaces via non-covalent adsorption.

4.5 Biomolecule recognition

The attachment of biomolecules capable of specific target recognition (*e.g.* ligands for membrane receptors/transporters, enzyme substrates, RNA/DNA, antibodies, or aptamers) to a NP surface is a universal strategy with many applications. Information on strategies for conjugation of NP and biomolecules (bioconjugation) can be found in an extensive (over 150 pages) review [177]. A variety of methods have been developed, including protein and DNA attachment to amine-reactive surfaces [255, 256], immobilization of biotin-activated proteins on streptavidin-coated surfaces [257], and specific attachment using an intermediate protein coupled directly to the surface (*e.g.* Protein A or Protein G) [258, 259]. Interest in this area continues unabated 30 years after the invention of the first protein microarray systems (for a great review of the "ligand assay" history, see [260]). In general, the choice of a suitable immobilization strategy is determined by the physicochemical and chemical properties of both the nanoparticle surface and the biomolecules. Several comprehensive reviews and books dealing with useful immobilization techniques were published in the past few years [261–266]. We focus here on antibodies, since they are excellent targeting agents due to their large epitope space and high affinity for their antigen. For example, they have the capacity to recognize disease biomarkers, *e.g.* on the surface of cancer cells, which makes antibody-coated NP useful for biomedical diagnostics or bio-imaging.

There are two general methods for generating antibody-coated NP: passive adsorption and covalent attachment. Passive adsorption is straightforward to conduct, cost efficient, and leads to the adsorption of protein layers (coronas) on the NP surface [179]. However, because the proteins are immobilized non-covalently, they can be removed and replaced by other biomolecules that exhibit higher affinity towards the NP

surface. Moreover, changes in antibody conformation or local pH can influence an antibody's isoelectric point and subsequently its electrostatic interactions with the NP surface, leading to more rapid desorption of the targeting antibody. Although this method of conjugation of biomolecules is not very popular for drug delivery systems, it is widely accepted in biomedical diagnostics. One of the best examples is the passive adsorption of antibody-coated Au NP on a gold surface for use in pregnancy tests [267].

The majority of covalent coupling strategies that are applied to NP utilize standard chemistry employing $-NH_2$/-COOH groups, which was first exploited for radio- and fluorescent-labelling of enzymes and proteins [268] (Fig. 5). One of the simplest examples of covalent conjugation of antibodies to NP involves the use of carbodiimide agents. For example, the zero-length 1-ethyl-3-[(3-dimethylamino)propyl] carbodiimide hydrochloride (EDC) reacts with carboxylated NP in the presence of sulfo-N-hydroxylsulfosuccinimide (sulfo-NHS) to form amine-reactive sulfo-NHS esters. The subsequent addition of antibodies results in coupling between the NP and primary amines on the antibody to form a stable amide bond. Unfortunately, the reaction is highly inefficient and thus requires a high excess of antibody. Typically, only about 1 to 20 % of the antibody used during the conjugation procedure can be coupled to the NP [269].

Another common approach to covalently coupling antibodies on the NP surface is based on two subsequent chemical reactions employing a variety of hetero- and homo-functional linkers [270]. The use of linkers is important, because they act as a spacer between the protein and the NP surface, thus avoiding denaturation of the typically expensive biomolecule and undesirable biomolecule-nanoparticle interactions [271]. There are many commercially available bi-linkers, for example glutaraldehyde [272], adipic acid [273], and succinic anhydride [274, 275]. Using glutaraldehyde, the biomolecule of interest is immobilized directly *via* Schiff base formation. In many other cases, additional reagents are required for activation. Unless the Schiff base linkage is stabilized by a borohydride-reduction step, the binding can be easily reversed. Furthermore, the chemistry of glutaraldehyde is rather complex and this compound is highly toxic. Gubala, *et al.* previously demonstrated the advantages of multivalent linkers such as dendrimers in bioconjugation reactions and compared the effect of using dendrimers of increasing generation number on NP stability [270]. Due to the uniform and hyperbranched nature of such starburst macromolecules, a significant increase in conjugation efficiency and reaction kinetics was observed [276].

It is also noteworthy that the synthesis of antibody-nanoparticle conjugates is usually plagued by low coupling efficiencies, resulting in the use of large quantities of antibody and high cost of reagents. Because nonspecific antibody coupling methods do not result in site-specific binding, the orientation of the antibodies on the NP surface is not controlled and the binding epitopes may not be accessible for target recognition. Approaches that attempt to control the site-specific orientation of antibodies focus on the Fc portion of IgG. For example, oxidizing the oligosaccharide moieties of the Fc region generates aldehydes, which can be reacted with amine- or hydrazine-terminated surfaces, resulting in the variable region of the antibody being oriented away from the ENM surface and available to recognize target molecules. Protein A can also be used for site-specific antibody immobilization, since it binds the Fc region of IgG. If immobilized to ENM surfaces, Protein A can bind the Fc region of antibodies to produce a bio-functionalized nanomaterial with the Fv region available for target recognition. Target recognition can also be improved by employing monoclonal antibodies, which bind a single specific epitope of an antigen. However, because monoclonal antibodies are expensive and protein coupling strategies are inefficient, polyclonal antibodies are often preferred, despite their reduced biomolecular recognition capability and potential for non-specific binding. The choice of antibody is therefore application-dependent. Regardless of the method used to attach biomolecules, it is important to evaluate the biological performance and the purity of the bio-functionalized NP. In doing so, the 'fraction of active biomolecules' on the NP surface (*i.e.* the fraction of biomolecules capable of target recognition) can be elucidated and the bioconjugation strategy effectively optimized [1]. This can be governed, in part, by the density and orientation of biomolecules on the ENM surface.

Liu *et al.* [277] took this into consideration when assessing the performance of enzyme-coated 18 nm gold NP. The authors studied protein-coated NP activity by (i) specifically orienting the enzyme (*E. coli* inorganic pyrophosphatase, EC 3.6.1.1) on the NP surface and (ii) varying the surface density of bound enzyme. The gold NP coated with specifically oriented enzyme exhibited 91 % activity relative to that of native enzyme in

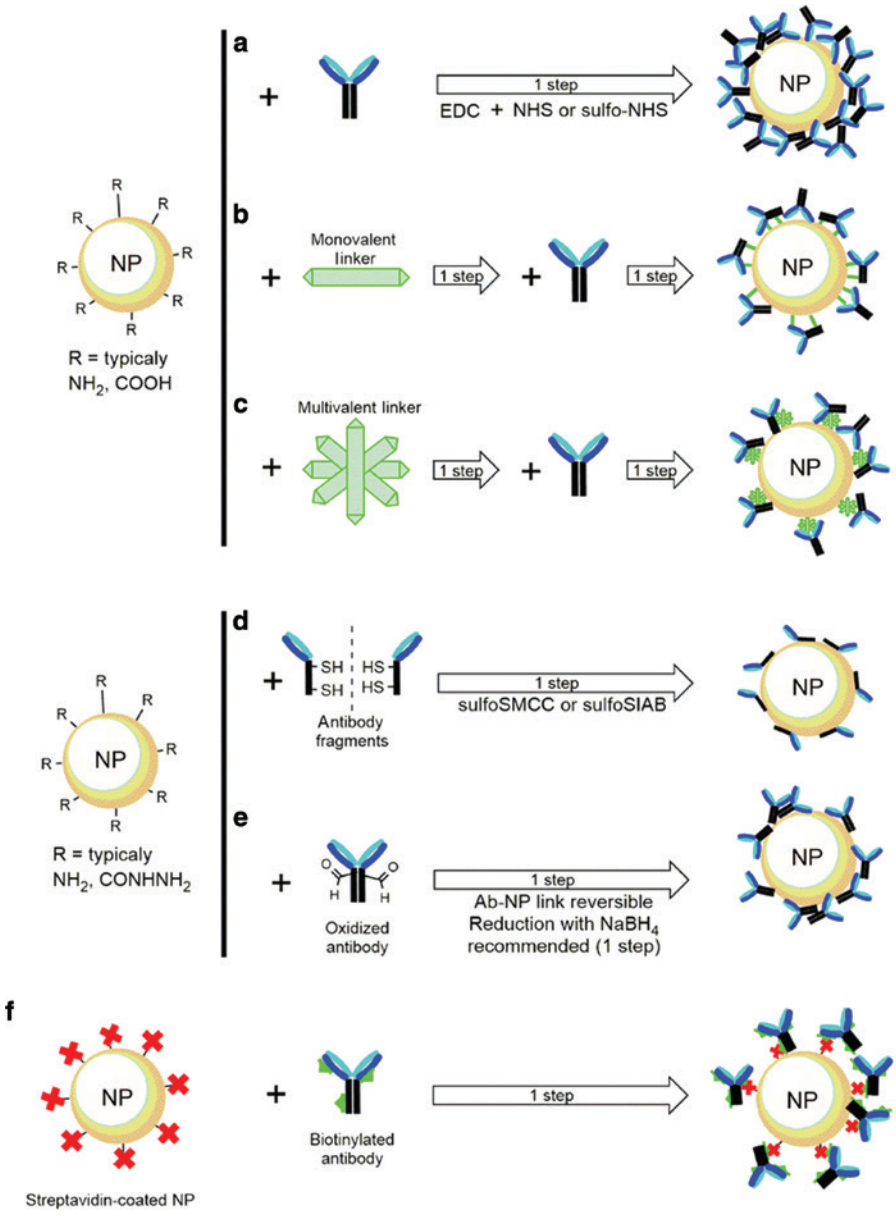

Fig. 5: Examples of the most popular chemical reactions for antibody--NP conjugation. a) One-step procedure using unmodified antibodies and coupling agent EDC or EDC/NHS (sulfo-NHS for better solubility in aqueous media); b) Two-step process using monovalent linkers such as glutaraldehyde and unmodified antibodies; c) Two-step process using multivalent linkers such as dendrimers and unmodified antibodies; d) One-step process using modified antibodies (fragmented by (2*S*,3*S*)-1,4-bis(sulfanyl) butane-2,3-diol, known as 1,4-dithio-D-threitol (DTT) or 2-sulfanylethan-1-ol, also known as 2-mercaptoethanol (2-MEA) – extra step) and heterofunctional bi-linkers such as sulfo succinimidyl 4-(*N*-maleimidomethyl)cyclohexane-1-carboxylate [sulfo-SMCC] or sulfo- succinimidyl (4-iodoacetyl)aminobenzoate [sulfo-SIAB]; e) One or two steps procedure using oxidized antibodies (usually by periodates); the antibody-NP linkage is reversible, therefore further reduction with borohydrides can be advantageous as it generates a stable covalent bond; f) One-step reaction between streptavidin-coated NP (many types are commercially available) and biotinylated antibody (also many types commercially available). Other types of site-specific antibody immobilization methods such as via His-tagged antibodies and NTA-Ni coated NP or via Protein A/G – coated NP (for binding to Fc region of immunoglobulins) are less common and therefore not illustrated in this figure. The cartoons used in this illustration show a solid NP, however NP are also often fabricated from porous material.

solution, while the NP with randomly oriented enzyme exhibited 58 % activity. It was also shown that saturating the NP surface with proteins did not greatly affect protein activity. The authors therefore concluded that biomolecule orientation had a larger influence on the activity of these bio-functionalized NP.

In summary, the conjugation of antibodies that are able to retain their specific activity and molecular recognition capacity on the nanoparticle surface still remains a challenging task. It is regrettable that some important factors, such as the effects of the cross-linker on the colloidal stability of the NP, the development of robust and simple methods of conjugating antibodies in an epitope-oriented fashion on the NP surface, and the antibody-binding efficiency of NP, have still not been fully addressed. This is alarming, especially since NP size and surface properties are considered important parameters for mediating the biocompatibility of new materials used in nanomedicine [33]. Exploring these important issues may lead to increasingly more robust methods for the conjugation of antibodies to NP surfaces.

5 Size-dependent features of nanomaterials

Some nanomaterials have novel properties that are not exhibited by the bulk material, leading to novel properties and applications [278]. Examples of such properties include light refraction of TiO_2 particles, unique optical features of quantum dots, novel catalytic or photocatalytic activities (*e.g.* of gold nanoparticles or nanoclusters), magnetic properties for imaging, or self-assembly of micelles to defined diameter. Because of the great importance of size in characterizing nanomaterials, it seems tempting to provide precise particle diameters at which the novel behavior is observed. However, that range is material-specific, meaning generally valid size limits for nano-specific characteristics cannot be given. Even if a nanosized material does not have nanosize-specific physiochemical features, the small size itself may be advantageous for body-close applications. These features include enhanced solubility, faster degradation in the organisms and environment, potentially higher catalytic rate due to the larger surface, as well as improved fluidity (*e.g.* when used in ointments). Table 1 lists examples of approximate sizes at which specific size properties have been observed for some nanomaterials.

A similar situation prevails with regard to size-dependent biological features that affect the fate of NP in a biological system (Table 2). For example, the pores for renal filtration have a diameter of about 8 nm.

Table 1: Size-dependent properties of ENM compared to bulk materials. The values for size limits are approximations and will vary with the nanomaterial composition and surface characteristics.

Approximate size range	Selected Material Properties
1 to 5 nm	Novel catalytic activities Self-restricted size of micelles
2 to 10 nm	Optical properties of quantum dots
20 to 30 nm	Changes in magnetic properties
16 to 40 nm	Changes in refractive index
1 to 100 nm	Range of superparamagnetism
100 to 500 nm	Properties tend to approach those of the bulk material

Table 2: Size-dependent features of ENM compared to bulk materials. The size-ranges are approximations and should be considered as a rough guide; material-dependent deviations often occur.

Size limits	Biological features relevant for NP transport in the organism
<0.8 nm	Pores of tight junctions between cells of biological barriers (*e.g.* intestine)
8 nm	Diameter of renal filtration pores
<50 nm	Cell uptake by pinocytosis in some cell types
~50 to 100 nm	Cell uptake by endocytosis
~100 to 200 nm	Cell uptake by pinocytosis possible
<300 nm	Intrusion of inhaled particles into the lowest (smallest) parts of the airways
~500 nm	Cell uptake by phagocytosis

Therefore, NP with diameters of up to 8 nm may be expected to be efficiently filtered. However, additional parameters, such as the surface charge, may strongly influence renal filtration. As a result, administered NP smaller than 8 nm do not necessarily appear in the urine, either because the kidney does not allow them to pass or because alternative elimination routes or storage prevail. Although ranges of up to 300 nm [279] or 500 nm [21] have been proposed to encompass important physiological behavior of ENM, the characteristic range for specific size-dependent behavior will vary with both the nanomaterial composition and the biological system of interest (see manuscript part 2).

6 Characterization methods for nanomaterials

The characterization of ENM is a key step to ensure the reproducible commercial production of materials with the same properties. Any attempt to compare the utility or efficacy of an ENM for a specific application or to assess its potential harmful effects requires that the material be adequately characterized after purification for all properties that are relevant to the specific end use in the relevant environment. Incomplete characterization of ENM is recognized as a major drawback in many publications, making it difficult to reproduce and validate experiments. Furthermore, purchased materials do not always conform to the material specifications provided and even subtle changes in synthesis, purification, storage, and/or handling conditions may cause significant variation in physico-chemical properties. The challenges associated with adequate characterization are compounded by the fact that there are many relevant nanomaterial properties and it is not always obvious which ones are important for a specific application. Moreover, the optimal method(s) for assessing the property of interest may not be known or the technique may not be readily available. Considerable effort is being expended to address this situation. There is a strong demand for a read-across system that will provide guidance on the characterization of specific classes of ENM, particularly from a regulatory perspective [280]. To date, this has been a challenging task, partly because there are many ways to organize ENM into classes, partly because the important properties usually depend on the specific application, and partly because the optimal method (or methods) for a particular property is not always well-established.

More than twenty physico-chemical properties of nanomaterials have been identified as important for the assessment of environmental, health, and safety risks for nanomaterials [281–283]. Generally, these properties are grouped into categories, such as composition and structure, size/shape, and surface properties. Table 3 summarizes the major properties. With a few differences for some less commonly measured properties that apply to a relatively small subset of nanomaterials, the categories in Table 3 are representative of the bulk of the literature. The characterization of nanomaterials presents a number of challenges [284] and it is recognized that, in most cases, multiple techniques are required to obtain reliable and complete information [284–286]. This is often difficult, since many academic and industrial labs may not have access to the range of methods and expertise necessary. Furthermore, different analytical methods for a specific property frequently do not measure the same parameter (*i.e.* the measurand is method-dependent), which makes comparisons difficult. In addition, the measurement conditions used in specific analytical methods can vary from laboratory to laboratory due to a lack of standardization. Another complication is that the properties of the material are often both time- and environment- (temperature, light, medium) dependent. Therefore, it is important to not only have a purified and well-characterized pristine material, but also to understand how its properties change with time and environment. Lastly, either the analytical sample preparation or the analysis technique (*e.g.* damage from electron or ion beams) may alter the property of interest.

6.1 Pre-analytics and sample preparation

Sample preparation is an important factor for consideration for all nanomaterial characterization methods. In all cases, the sample must be carefully purified to remove all excess reagents or undesired by-products resulting from either the initial synthesis or surface modifications. The purification method varies depending

Table 3: Methods for characterizing nanomaterials.

Nanomaterial property[a]	Analytical Method	Comments
Composition/ presence of contaminants	Elemental analysis Nuclear magnetic resonance Mass spectrometry (coupled with gas or liquid chromatography or inductively coupled plasma) Raman and Infrared spectroscopy UV-VIS and fluorescence spectroscopy Optically coupled plasma-optical emission spectroscopy Endotoxin and pyrogen assays	Bulk chemical composition Presence of surface coatings, dispersants or stabilizers Presence of impurities/contaminants Detection of endotoxin and pyrogen impurities is important for toxicological evaluations
Crystal structure/ Crystallinity	X-ray diffraction Nuclear magnetic resonance	X-ray diffraction also gives crystal size
Primary particle size, particle size distribution	Electron microscopy Scanning probe microscopy Light scattering (dynamic, multiple or static light scattering) Nanoparticle tracking analysis Differential mobility analysis (scanning mobility particle sizing) Centrifugal liquid sedimentation (analytical ultracentrifugation) Gel filtration Scanning ion occlusion spectroscopy Field flow fractionation Small angle X-ray scattering	Samples can be liquid suspensions, or dry or aerosol particles, depending on the method Size is method dependent (see Table 3) Methods can be classified as: – particle counting (both imaging and non-imaging methods), – ensemble (all particles in sample are measured at same time) or – separation/fractionation (particles are separated based on size, prior to analysis by either particle counting or ensemble methods)
Shape, aspect ratio	Electron microscopy Atomic force microscopy Light scattering methods	Microscopy methods are best suited to identifying particle shape and aspect ratio Light scattering data can be used in some cases
Particle association	Electron or scanning probe microscopy UV-VIS or fluorescence spectroscopy	Microscopy methods provide direct information on association of particles Most other particle sizing methods do not distinguish between large particles and clustered/associated particles Optical spectroscopy provides information in some cases
Dispersibility	Particle sizing methods Turbidity Rheological measurements	Changes in dispersibility are generally assessed by light scattering methods or turbidity or rheology measurements
Surface area	Gas or liquid adsorption isotherms (Brunauer-Emmett-Teller)	Adsorption method is only suitable for dry samples; sample association is a limitation for some nanomaterials
Surface Charge	Measurement of electrophoretic mobility by either optical or acoustic methods	Zeta potential calculated from electrophoretic mobility
Surface functional groups	Nuclear magnetic resonance Secondary ion mass spectrometry Raman and Infrared spectroscopy X-ray photoelectron spectroscopy Auger electron spectroscopy Elemental analysis Titration (acidic/basic groups) Fluorescence and UV-VIS assays Ellipsometry Detection using antibodies	Important for quantifying extent of surface modification, type of functional group, presence of surface contamination Most of these methods (with exception of SIMS and optical assays) are not generally used for analyzing adsorbed proteins or covalently attached biomolecules

Table 3 (continued)

Nanomaterial property[a]	Analytical Method	Comments
Chemical reactivity/ stability	A wide range of methods can be used to assess reactivity by measuring final products (see composition) and their rates of formation Thermogravimetric analysis for thermal stability	Includes catalytic reactivity, photochemical reactivity, thermal stability Dissolution of some nanomaterials may occur in aqueous or biological media or in environmental samples

[a]Mechanical, electrical and optical properties are important for many nanomaterial applications but are not included here.

on the material composition with dialysis through semi-permeable membranes with an appropriate cut-off, chromatography, centrifugation and ultrafiltration being among the most commonly used techniques. It is important to ensure that the starting sample is homogeneous and that the sub-sample to be analyzed is representative of the overall material. One of the first considerations is whether the sample is obtained as a dry powder, a liquid suspension, or an aerosol, since this will dictate the choice of appropriate methods. In many cases, a dry sample may require dispersion in a solvent prior to analysis; in such cases the dispersion method and the solvent have to be selected and optimized. For aqueous suspensions, factors such as the buffer, the pH, and the presence of salt can all have a significant effect on the nanomaterial properties. The use of salt concentrations that have physiological ionic strength may cause the association of nanomaterials due to the screening of electrostatic charge on the particle surface. The concentration of the ENM is also important, as it may control the association of the particles. For aerosol samples (generally for detection/characterization of environmental or workplace contaminants), the collection method must be carefully chosen to ensure a representative sampling of the material at adequate concentrations for the analytical method to be used. Additional method-specific factors are discussed in the sections below.

The methods summarized in Table 3 are applicable to most pristine ENM (either as dry materials or suspensions), although in some cases the sample size requirements may be a limitation. However, many of the characterization methods are challenging or impossible to utilize for nanomaterials in the more complex environments typical of biological or environmental samples. Finally, there are typically multiple methods that can be used to measure a specific physicochemical property. The selection of the "best" method (or methods) for a specific ENM will be based on compromise between the following factors: cost, availability, skill of operators, required resolution/sensitivity, sample format, and accuracy/precision required for a specific end use of the ENM. In summary, it should be stressed that the selection of the proper method to obtain a homogeneous sample and the appropriate analytical method are key to obtaining reliable data.

6.2 Composition/purity/structure

The composition of a nanomaterial is one of the most basic properties of interest and can frequently be measured by techniques such as elemental analysis or spectroscopic methods that are typically employed for bulk materials (Table 3). This is reasonably straightforward for single-element or single-compound nanomaterials but is more challenging for core-shell particles (*e.g.* QD or silica-coated NP). In these cases, a combination of bulk and surface sensitive methods may be required for compositional analysis. Note that, although the chemical composition is generally defined by the synthesis method employed, the presence of impurities or contaminants frequently has a major impact on the behavior of the material. The large surface area-to-volume ratio of nanomaterials increases the possibility that the impurity is near or on the surface, where it may more readily modify the properties of the nanomaterial. In some cases, the amount of impurity present may be below the detection limit of a specific analytical method.

Nanoparticles are commonly synthesized with a variety of surface coatings to either stabilize or disperse the material, which must also be taken into account. The amount of surface coating can vary considerably

depending on the sample history. It should be noted that additives used to stabilize or disperse the material may be more challenging to detect and quantify than covalently attached surface functional groups, which typically do not change with the nanomaterial environment. Of particular importance for biological studies is the presence of endotoxins (pyrogens) which are common contaminants and can lead to toxicity effects that have nothing to do with the nanomaterial itself. The suitability of several commonly used tests for endotoxins has been evaluated, highlighting the fact that nanomaterials interfere with some of the assays [287, 288].

X-ray diffraction is the most widely used method for analyzing the structure of crystalline materials. The lattice spacing can be determined from the angle of constructive interference when X-rays scatter from crystalline materials. The powder method (Debye-Scherrer) is used for nanomaterials which are generally studied as dry powders. Analysis of the peak position and intensity is used to identify and quantify the phase composition of the sample. The general challenges associated with obtaining structural information for nanomaterials using X-ray diffraction and other surface characterization tools have been discussed [289].

6.3 Shape, size and size distribution, aspect ratio

It is generally recognized that measurements of the size, size distribution, and shape (including aspect ratio for non-spherical particles) are among the top priorities for most, if not all, nanomaterials. There are three general approaches for obtaining size distributions (see Fig. 6). The first relies on particle counting methods, typically electron or scanning probe microscopies, which provide details on the shape of particles and (in some cases) the presence of associated particles. The second approach relies on ensemble methods that measure all particles in the solution. A third classifying or fractionation approach involves the pre-separation of nanomaterials based on their size prior to analysis by either particle counting or ensemble methods and is particularly useful for samples with broad size distributions. As reviewed recently, there are trade-offs for each approach [290, 291]. Careful consideration of the sample characteristics, the time and resources available, and the required measurement accuracy are necessary to select the most appropriate method, or frequently, combination of methods. Table 4 summarizes the various particle sizing methods according to these three categories.

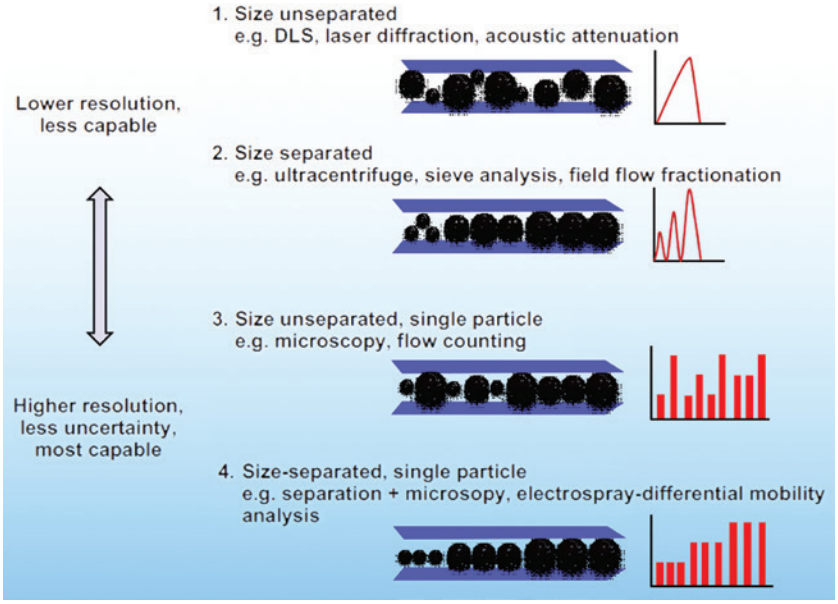

Fig. 6: General categories of particle sizing methods. Higher resolution methods usually assess particles individually, lower resolution techniques do not separate particles and provide an average number from the bulk. Adapted from [290].

Table 4: Methods for determination of size and size distributions for nanomaterials.

Method	Measurand	Size range	Sample environment	Particle concentration measurement	Comments
Particle counting methods (number weighted size distributions)					
Scanning electron microscopy	Length, width, shape (2-D)	Several nm – mm	Surface-adsorbed particles, vacuum[a]	no	Sample staining may be required for organic particles
Transmission electron microscopy	Length, width, shape (2-D)	0.5 nm – 10 μm	Surface-adsorbed, particles vacuum[a]	no	Sample staining may be required for organic particles
Atomic force microscopy[b]	Length, width, height (3-D)	1 nm – 100 μm	Surface adsorbed particles in air, liquid or vacuum	no	Tip convolution effects for lateral measurements
Nanoparticle tracking analysis	Equivalent hydrodynamic diameter (diffusion)	10 nm – 600 nm	Liquid suspension	yes	Sensitivity to small particles depends on scattering intensity; limited to particles that do not sediment during measurement time
Scanning ion occlusion spectroscopy	Volume equivalent diameter	50 nm – 100 μm	Liquid suspension	yes	Same principle as Coulter counting for larger particles
Differential mobility analysis (scanning mobility particle sizing)	Electrical mobility diameter	3 nm – 1 μm	Aerosol particles	yes	SMPS is DMA used with a condensation particle counter in continuous scan mode
Ensemble Methods (intensity-weighted distributions)					
Dynamic light scattering	Equivalent hydrodynamic diameter	10 nm – 2 μm	Liquid suspension		Cumulants analysis gives mean diameter and polydispersity index for samples with reasonably uniform sizes; other analysis methods used for bi or multi-modal distributions
Small angle X-ray scattering	Equivalent scattering diameter	1 nm – 150 nm			
Fractionating (or classifying) methods					
Centrifugal liquid sedimentation (Analytical ultra-centrifugation)	Equivalent hydrodynamic diameter	1 nm – several μm	Liquid suspension	yes	Detection by turbidity, UV-vis absorption or X-ray absorption
Field flow fractionation	Equivalent hydrodynamic diameter	1 nm – 100 μm	Liquid suspension	yes	Various methods and detection systems are available, including UV-vis absorption, refractive index, multi-angle light scattering, dynamic light scattering
Cascade Impactor	Mass-based aerodynamic diameter	10 nm – 10 μm	Aerosol particles	yes	Ability to measure full distribution of aerodynamic diameter is limited by number of collection stages

[a]Cryo-transmission electron microscopy and environmental scanning electron microscopy are also available and are useful for fragile samples and for alternate environments, respectively.
[b]Scanning tunneling microscopy also provides size information, although its suitability for measuring particle size distributions is limited.

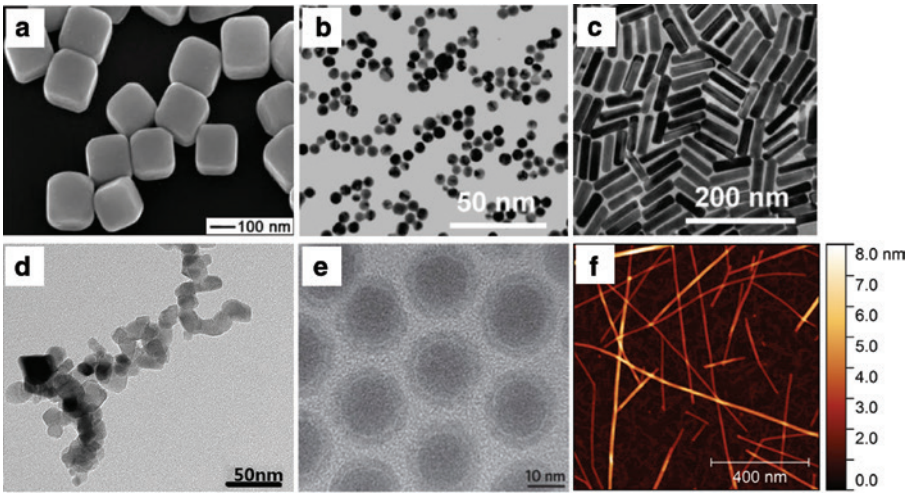

Fig. 7: Images of various types of ENM. (a, b, c) TEM images of gold nanoparticles with 3 different shapes (cubes [295]; spheres and nanorods imaged on Formvar grids [296]). (d, e) TEM images of titanium dioxide nanoparticles [297] and core-shell iron oxide nanoparticles [298]. (f) AFM image of polymer wrapped carbon nanotubes on mica with *z*-scale as color bar [299].

6.3.1 Microscopy particle counting methods

The shape and size of nano-objects can be assessed by either scanning or transmission electron microscopy (SEM, TEM), or by atomic force microscopy (AFM), all of which image individual particles and measure their size (length, width, or height) and shape (see Fig. 7). Based on the spatial resolution (see size range column for microscopy methods in Table 3) and the ability to deal with associated and/or non-spherical particles, microscopy (often TEM) is frequently the primary characterization method for obtaining size distributions. Microscopy is the only method that allows for the direct visualization of the shape and size of individual particles (and associated particles). Nevertheless, this is neither a rapid nor a straightforward process. Both electron microscopy and AFM require the sample to be deposited on a surface or grid and yield the most reliable information for well-dispersed particles. Thus, sample preparation, including the dispersion of the initial dry samples and deposition on a suitable surface, often requires considerable optimization. The most common methods for sample preparation include (1) incubation of dilute samples of nanomaterials with an atomically flat surface or electron microscopy grid followed by washing, (2) drop-casting and drying, and (3) spin coating [292–294]. Although most preparation methods have the potential to select for a specific size or shape of particles during the sample deposition process, thereby limiting the ability to obtain data for a representative sample, this possibility has rarely been examined. The use of surfaces with a charged coating is a common approach to ensure the immobilization of charged particles [292] and to help minimize association of particles. Although microscopy can provide information on clusters of particles, it is not usually possible to determine whether the associated particles are present in the initial sample or whether they are formed during sample deposition.

In addition to optimizing the sample preparation to ensure representative sampling and well-dispersed nano-objects, it is important to ensure that the sample is not damaged by the imaging conditions, for example by the intensity of the electron beam or the scanning action of an AFM probe. Obtaining size information on non-uniformly sized samples may require collecting images on different length scales to adequately resolve small and large particles, adding to the time and resources required. The measurement of a large number of individual particles (n) is required to determine the particle size distribution, with non-uniformly sized samples and/or lower measurement uncertainty requiring larger n. The ability to distinguish between two size distributions depends on the width of the distribution and the level of confidence required. The length of time required to analyze the dimensions of individual particles (excluding clustered particles) is frequently considerably longer than that required for data acquisition and is a significant limitation to acquiring size distributions based on large numbers of particles by microscopy. Automated approaches have been

employed in some cases, although so far with most success for well-separated spherical particles that have relatively narrow size distributions. Finally, particle counting methods can never interrogate more than a very small fraction of the sample, so it is important to ensure representative sampling, for example by splitting the initial sample and measuring multiple parts. Microscopy data is typically plotted as histograms that illustrate the distribution of length and cross-section (width or height); the mean (number average), standard deviation (as a measure of the width of the distribution), and number of particles analyzed are reported. More advanced analysis methods that measure other parameters (aspect ratio, perimeter, circularity, *etc.*) are sometimes used for non-spherical particles and can be useful for distinguishing multiple populations within non-uniformly sized samples. Methods for particle size analysis and sampling for microscopy, as well as information on the general and technique-specific issues that are often encountered are summarized in a number of standards [300–303].

6.3.2 Particle counting by non-imaging methods

Nanoparticle tracking analysis (NTA) is a potentially useful alternative particle counting method. NTA measures the light scattered by particles in suspension as they diffuse within a focused laser beam that is aligned so that only particles in the focal plane of the collecting optics are illuminated [304]. The motion of individual particles is recorded using a charge-coupled device camera with high time resolution and the trajectory of each particle is calculated as the mean squared displacement, from which the diffusion coefficient can be determined (Fig. 8). The equivalent hydrodynamic diameter is obtained using a modified Stokes-Einstein equation that accounts for three-dimensional diffusion [305]. Since all particles in the laser beam are tracked separately, this method provides a number count-based distribution (unlike ensemble light scattering methods) and can deal with non-uniformly sized samples. There are several requirements for obtaining reliable data, including optimization of the particle concentration and light intensity so that individual particles can be followed over an adequate tracking length. This may be particularly challenging for highly non-uniformly sized samples. The data quality is affected by the scattering intensity from individual particles, which is in turn controlled by their composition. Finally, data analysis assumes spherical particles, a criterion which limits the applicability to non-spherical particles, and associated particles will appear as a single large particle, in contrast to microscopic methods which can often distinguish between individual and associated particles. Nevertheless, NTA is a time and cost-effective alternative to microscopy measurements for some samples and its ability to provide number-based distributions, even for uniformly sized samples (see Fig. 8, in which 100, 200 and 300 nm particles are clearly distinguishable), is a significant advantage over ensemble methods such as dynamic light scattering (see below) [306].

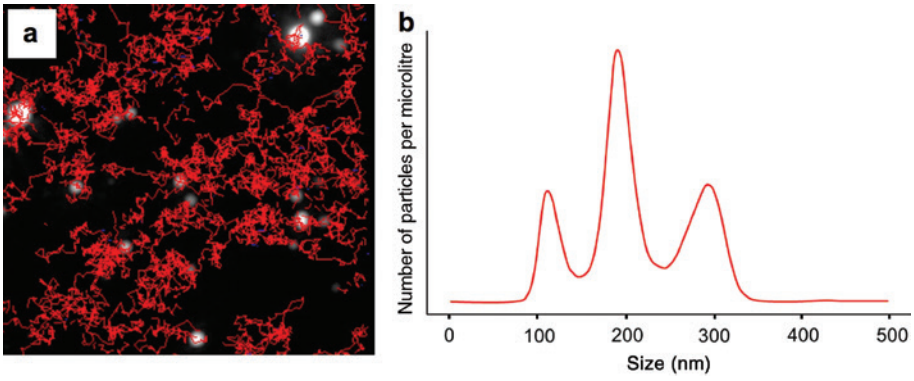

Fig. 8: Nanoparticle tracking analysis for a sample containing 3 sizes of polystyrene beads. The software tracks many particles individually (a) and uses the Stokes Einstein equation to calculate their hydrodynamic diameters (b). The system has higher resolution output with more detailed size distribution of particles in a non-uniformly sized sample and provides the particle concentration. Source: EMPA, Switzerland.

Scanning ion occlusion sensing (SIOS, also known as tuneable resistive pulse sensing, TRPS) is an emerging particle counting method that is based on the same principle as Coulter counting, but is applicable to nanometer-sized particles [307]. The method measures the change in resistance when a particle passes through a pore or channel; the change in resistance is proportional to the volume of electrolyte displaced and hence to the particle volume, which in turn is proportional to particle size. SIOS requires non-conductive particles and dispersion of the sample in an electrolyte. The magnitude of the change in resistance is proportional to the particle-to-pore volume ratio, so that the sensitivity can be adjusted by varying the pore size. If the pore size is narrow but the particle still traverses it, then the volume of electrolyte displaced is large. Thus, the change in resistance detected, observed as a 'pulse', is distinguishable from background signal. Particle concentrations are obtained from the pulse frequency (*i.e.* the number of particles that traverse the pore per unit of time). SIOS provides volume-based size distributions based on the diameter of an equivalent sphere, although it is possible to model the behavior of non-spherical (elliptical) particles. Similar to NTA, the main advantage of SIOS is the ability to provide a number-based size distribution. However, the analysis of NP less than 100 nm can be challenging, as associated NP or multiple NP attempting to traverse the pore at the same time can result in pore blockage. When employing a larger pore size, the pulse generated by a single NP may not be discernable from background due to insufficient volume displacement.

6.3.3 Ensemble methods

Ensemble methods interrogate the entire sample, thus avoiding the sampling problem encountered with particle counting methods, and are generally rapid and easy to use. Nevertheless, they usually have lower resolution than particle counting approaches, often yield only an average size and do not work well with non-spherical or non-uniform nanomaterials. Despite these limitations, ensemble methods are widely used for routine measurements and are suitable for assessing batch-to-batch reproducibility of samples.

Dynamic light scattering (DLS) is the most commonly employed ensemble method and measures the time-dependent fluctuations in intensity of light scattered from particles suspended in liquid and undergoing Brownian motion. These intensity fluctuations are plotted as a correlation function from which the translational diffusion coefficient, D_t, can be calculated using the Cumulants method [305, 308]. The Stokes Einstein equation is then used to calculate the mean hydrodynamic diameter, d_h. For a non-spherical particle, one obtains the equivalent hydrodynamic diameter, which is the diameter of a rigid sphere that diffuses at the same rate as the analyte particle. The intensity-weighted equivalent hydrodynamic diameter, d_h, of solvated particles estimated from DLS will almost always differ from the diameter measured by microscopic methods. For spherical particles, the differences are primarily due to the electrical double layer, whereas the situation will be more complex for non-spherical particles. The scattering intensity is proportional to r^6 (where r is radius of the scattering particle), which means that the scattered intensity from a 100 nm particle will be 1 million times larger than that from a 10 nm particle. DLS is compatible with any type of nanoparticle that does not absorb at the laser wavelength and that gives a stable colloidal suspension, and the minimum detectable size can be as small as a few nm for materials with a large scattering cross section. Usually, samples are filtered to eliminate large clusters of particles and are measured in the presence of modest salt concentrations to minimize the electrical double layer.

The fit of the correlation function using the Cumulants method also provides the polydispersity index, PI, which is a dimensionless measure of the broadness of the size distribution. DLS works well for uniformly sized samples (polydispersity index <0.1), but is not recommended for samples with broad size distributions [285]. Although a range of algorithms have been used to fit the correlation curve to extract multiple components for non-uniformly sized samples, there is so far no generally accepted method for analyzing such samples. DLS provides intensity-weighted distributions that differ from the number-weighted distributions obtained from particle counting methods. The intensity-weighted distribution provided by DLS can be converted to a volume distribution using Mie scattering theory and the refractive index of the particle. The volume distribution has the advantage of more clearly showing signals due to small particles that have low scattering intensity and is shifted to lower apparent diameter. Although further conversion to a number-based distribution (to compare

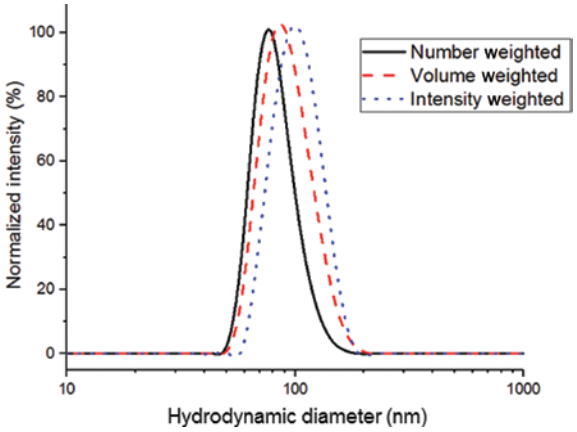

Fig. 9: Comparison of intensity, volume and number-weighted size distributions determined by dynamic light scattering for silica nanoparticles. The nanoparticles have an average hydrodynamic diameter of 98.9 nm based on intensity weighted data and a diameter of 82.6 nm from TEM. The *x*-axis is on a logarithmic scale. Source: National Research Council Canada.

to particle counting methods) is possible, each conversion leads to additional sources of error (see Fig. 9). Multi-angle light scattering (dynamic or static) has been employed to overcome some of the issues associated with DLS (for example the requirement to avoid multiple scattering events), but is still not widely used [309].

Small angle X-ray scattering (SAXS) provides information on the size and shape of particles in suspension [310]. The particle and the liquid phase must have different densities and the particle concentration must be low enough to avoid particle-particle interactions. The scattering data can, in principle, be fit to extract both size and shape information, but generally only for relatively uniformly sized samples of spherical particles that have a uniform density throughout (*i.e.* core-shell particles are problematic). As for other ensemble methods, SAXS is relatively fast and does not suffer from sampling issues. Neutron scattering has similar capabilities, but is only accessible at national facilities.

6.3.4 Fractionation or classifying methods

Fractionation methods separate particles of different sizes prior to their analysis by either an ensemble or particle counting method. Although these techniques are typically less reproducible and more difficult and time-consuming than ensemble methods such as DLS, the ability to resolve non-uniformly sized samples is a significant advantage. However, these methods are not able to distinguish between primary and associated particles; they separate and classify particles based on an equivalent spherical diameter [290].

Centrifugal liquid sedimentation (CLS) and analytical ultracentrifugation fractionate particles based on their rate of sedimentation induced by centrifugal forces. The rate of sedimentation depends on the particle density and size, with the Stokes equation used to calculate the Stokes diameter from the time required for the particle to travel a specific distance at a given angular velocity. This requires the particle density (which is assumed to be the same for all particles) as well as the density and viscosity of the liquid. A further constraint is that the density of the particles must be significantly higher than that of the liquid in order for sedimentation to occur. It is also important to note that, similar to DLS, the Stokes equation calculates the equivalent spherical diameter; non-spherical particles will orient to give maximum drag and will therefore settle at slower velocities. CLS typically uses one of two possible geometries. With the disc or line-start method the sample is introduced as a thin layer on top of the spinning liquid, whereas in the homogeneous method particles are initially distributed uniformly throughout the liquid. Commercial CLS detection systems use turbidity, optical absorption, or X-ray detection to monitor sedimentation of the particles. This method has an advantage over ensemble methods for non-uniformly sized samples and provides data that is more similar to a number-based distribution than the intensity-weighted data obtained from DLS.

Field flow fractionation (FFF) separates particles based on changes in their mobility as a fluid is pumped through a narrow channel in a laminar flow. The fluid moves more rapidly in the centre of the channel than at

the edges and a field (gravitational, cross-flow, electric) is applied perpendicular to the flow direction, which pushes particles to the edge of the channel. Smaller particles diffuse more rapidly against the applied field towards the centre of the channel and will be eluted more rapidly. FFF separates particles according to their equivalent hydrodynamic diameter and requires calibration with standard samples with the same properties to provide size information from elution times. Since such standards are rarely available, FFF is typically combined with a detector (light scattering, refractive index, UV absorbance) for on-line size measurement. Fractions can also be collected and then analyzed by any of the particle counting methods. FFF as a fractionation method is well-suited to non-uniformly sized samples, but can only provide information on associated particles when combined with a microscopy method that can distinguish clusters from primary particles.

A cascade impactor separates airborne particles based on their aerodynamic diameter, using the inertial separation of solid or liquid particles in the gas phase. Since this method requires aerosolized particles, it is most frequently used for aerosol research or inhalation studies. Aerosolized particles are forced through a series of impaction plates arranged in order of decreasing particle size. At each individual stage particles in the aerosol stream with sufficient inertia will be trapped on the stage collection plate, while smaller particles with insufficient inertia will pass on to the next stage. Particles collected at each stage are analyzed gravimetrically or used for size or composition analysis. This method can use a large range of stages to cover a wide dynamic range, but it is prone to errors due to stage overlap and particle trapping on non-plate surfaces, both of which make it difficult to obtain accurate particle size distributions. Furthermore, the tendency for dry particles to associate is a limitation for many types of nanoparticles.

6.4 Comparison of particle sizing methods

The various particle sizing techniques described above are based on different physical principles and provide method-defined sizes. Since different methods give different sizes, it can be challenging to make comparisons. Examples include the differences between intensity- *vs*. number- *vs*. volume-based measurements, as well as between the diameter of a dry particle as measured by microscopy and the hydrodynamic diameter measured by methods that analyze particles in suspension. It is still relatively rare to use multiple methods for routine characterization, although combinations of an ensemble method with a particle counting approach are becoming more common. However, there are now a few detailed studies that compare results obtained using different techniques for the same samples. One recent interesting example used six different techniques to examine silica particles with sizes between 100 and 400 nm (see Fig. 10) [286].

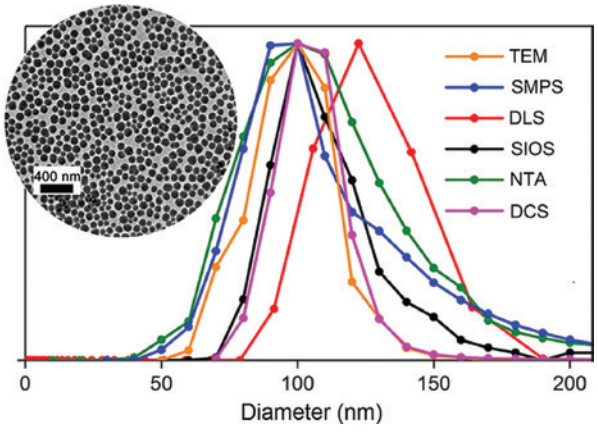

Fig. 10: Number-weighted particle size distributions for nominally 100 nm silica nanoparticles measured by 6 analytical methods: Transmission electron microscopy (TEM), scanning mobility particle sizer spectrometer (SMPS), dynamic light scattering (DLS), scanning ion occlusion sensing (SIOS), nanoparticle tracking analysis (NTA), differential centrifugation sedimentation (DCS). Reproduced with permission from ref [286].

The authors reported that, despite the different measurands for the various techniques, the reported size distributions were all within one standard deviation for these spherical particles. They also highlighted the crucial importance of adequate optimization of the sample preparation method and measurement conditions, the importance of reporting full particle size distributions, and the need for more reference materials for the validation of protocols and measurement results. Related examples looking at a more limited number of techniques have emphasized similar conclusions [285, 294, 311]. So far, most measurements of this type have focused on spherical particles with relatively uniform particle sizes. Similar studies for more disperse samples and non-spherical particles would be very beneficial to better understand the key differences in the various particle sizing approaches.

6.5 Dispersion and particle association

Although dilute solutions of nanomaterials usually contain a relatively large fraction of isolated primary particles, dry nanomaterials exist primarily as strongly associated clusters of particles. In some cases, the associated particles may be very difficult to break apart without danger of disrupting the constituent particles [291]. Dry nanomaterials can sometimes be redispersed by simple dilution and shaking in an appropriate solvent (possibly with a stabilizing agent). However, usually more energy is required and the application of ultrasound to a suspension of particles is the most common way to separate associated particles. The energy and time required to redisperse nanomaterials will depend on the type of sample, its environment, and the instrument used. Guidelines for standardizing the measurement of sonication power and reproducible preparation of nanomaterial samples by sonication have been reported [312]. It is important to minimize the energy applied, since excess energy may cause chemical damage or break apart primary particles.

A 2012 report concluded that there is so far no method that can reliably distinguish whether a large particle is a cluster of primary particles or a single particle, while at the same time measuring the size of large numbers of constituent particles [291]. In some cases, clusters can be identified by microscopy, although it may not be possible to ascertain whether they were present in the initial sample or were formed during sample preparation. Repeating size measurements using a rapid method such as DLS before and after application of sample dispersion methods can frequently give some information on changes that are related to breaking up clustered particles. Nevertheless, the measurement of sizes and the extent of association for complex samples that contain mixtures of primary particles and clusters remains a significant challenge. Unfortunately, such complex "real-world" samples are more common than dilute solutions of well-dispersed nanomaterials.

6.6 Surface properties

The specific surface area of ENM provides one measure of confirming their assignment as a nanomaterial and provides an estimate of the surface area available for modification to incorporate functionality for specific applications. The specific surface area of solids is typically determined by measuring the amount of physically adsorbed gas according to the Brunauer, Emmett, and Teller (BET) method for interpreting gas adsorption isotherms [313, 314]. This method allows the determination of overall specific external and internal surface area of dispersed (*e.g.* dry nanomaterials) or porous solids; dry samples are degassed at elevated temperature (above 100 °C) before measuring adsorption of gas, typically nitrogen or argon. Although the BET method has been applied to some nanomaterials, there may be complications due to particle association when samples are degassed at high temperatures, since the measured surface area of tightly associated particles is not equal to surface area of primary particles [291, 315]. It is also important to keep in mind that porous materials may have very high surface areas, without being nanomaterials, based on the size of individual particles.

6.6.1 Surface charge

Measurement of the zeta potential is one of the most common methods to determine the surface charge for NM. Zeta potential is defined as the difference between the electrical potential of the bulk liquid and that of the stationary layer of fluid attached to the dispersed particles (*i.e.* the slipping plane, which is the region of the liquid-solid interface where the liquid starts to slide relative to the surface under the influence of shear stress) [316]. Zeta potential is calculated using appropriate theoretical models from an experimentally measured parameter, such as the electrophoretic mobility [316]. A potential is applied across two electrodes in the sample cell and the movement of charged particles towards the oppositely charged electrode (cathode or anode) is measured as a function of the applied electric field. Particle mobility is typically measured by electrophoretic light scattering, which measures mobility from the Doppler shifts in the frequency of scattered light from particles moving in the applied field [316–318].

Zeta potential is a useful parameter for assessing the stability of colloidal suspensions and studying adsorption on particles. A key consideration is that the calculated zeta potential is a function of both the particle and its surrounding solution and will therefore depend on the pH, temperature, particle concentration, ionic strength of the dispersing solution and the presence of polyvalent ions. As a general guideline, solutions with negatively charged particles that have zeta potentials of –30 to –40 mV are considered moderately stable while values of –60 to –80 mV indicate very good stability [318].

6.6.2 Surface chemistry

The surface of nanomaterials is frequently functionalized to increase the stability of the material and prevent particle association, to improve its compatibility with other materials, or to add targeting moieties. The surface chemistry can dramatically change the properties of the nanomaterial, including its stability, surface charge, hydrophobicity/hydrophilicity, and, in some cases, size and morphology and association. Surface functional groups are also critical for controlling the behavior of the material when/if it is released to the environment, when it is used for biological purposes, or when it is incorporated in more complex materials. Despite the importance of surface functional groups, their quantitative analysis remains a considerable challenge. Although there are many possible methods that can be used, it is still relatively rare that more than one method is employed and even rarer that results are validated with multiple methods.

There are a large number of methods (see Table 3) that can be used to detect and quantify surface functional groups on nanomaterials. The chosen method is dependent on the nanomaterial state (dry powders, colloidal suspensions or airborne particles) and the various methods have quite different sensitivities. Some methods, such as X-ray photoelectron spectroscopy (XPS), are typically applied to planar surfaces rather than nanomaterials, and others are more generally used for bulk materials. Two recent reviews have summarized the more commonly applied approaches [284, 300]. One recent report has provided an interesting comparison of XPS, solid-state NMR, and fluorescence for the quantification of surface carboxylic acids groups [319]. The comparison of methods with overlapping sensitivity ranges provided validation of the methods and is a useful first step towards reference materials for surface quantification.

6.7 Matrix-related restrictions

The methods described above are mostly appropriate for purified, pristine nanomaterial, but they are of limited or no use in complex matrices, such as soil, food, consumer goods, or body fluids. In some cases, this is because the nanomaterial is present in relatively low amounts and must be concentrated prior to analysis. In other cases, the nanomaterial may be present in adequate quantities for detection and analysis but must be extracted from the matrix because other components of the sample are incompatible with the analytical method. The extraction and concentration methods needed are frequently unavailable or untested for specific combinations of nanomaterial and matrix. For biological samples, alternate approaches, such as

labeling methods with antigens that can be detected with antibodies or with fluorophores, may be necessary to detect and quantify nanomaterials. In experimental settings, labelling with (radioactive) isotopes can also be employed. Although these approaches may allow for qualitative, or sometimes even quantitative, detection of the nanomaterial, it is challenging to obtain detailed information on the nanomaterial composition unless a relatively pure sample can be obtained free from the environmental or biological matrix.

7 Discussion and closing remarks

Engineered Nanomaterials have attracted significant attention due to their unique and potentially revolutionary properties. The number of applications in which ENM are expected to enable economic and technological advances is still growing very rapidly. Nanotechnology-based (or enabled) products are making their way to the marketplace, despite concerns about the safety of the synthetic nanomaterial or the products in which it is incorporated. In this first document, *Engineered Nanomaterials and Human Health: Preparation Functionalization and Analytical Characterization*, we provided a brief overview of the terminology for nanomaterials, including the inconsistent use of the term "nano", and then reviewed the generally accepted methodologies for the synthesis, functionalization, and characterization of some of the common types of ENM.

The wide variety of synthetic methods that have been developed now makes it possible to synthesize many types of ENM with specific and well-controlled shape, size, and dispersity [298]. However, the range of methods that have been extended to commercial or industrial scale production is considerably more limited and environmentally-friendly "green" synthetic methodologies are also lacking. There has been an exponential growth in the number of publications on the synthesis of new ENM with potentially novel properties and applications over the last several decades. Nevertheless, many studies fail to adequately characterize the new material or provide a comprehensive investigation of its biological behavior. Many studies also fail to document whether the new material has significant advantages over existing materials. When ENM are explored as novel drug delivery systems, systematic attention should be paid to pharmacokinetic and pharmacodynamic requirements in addition to loading yields and *in vitro* sustained release profiles, which are generally all that is provided in published investigations.

Functionalization is essential for most ENM, either to control particle stability and association or to impart biocompatibility or targeting to specific biological pathways. Reproducible control over the density and orientation of surface functional groups remains a significant challenge. Many functionalization strategies are based on existing methods for surface modification or bioconjugation, but their application to ENM may be problematic due to the heterogeneity in particle size, surface composition, and the effects of particle curvature. Some strategies for surface modification give low yields and difficult-to-purify materials. Variation in surface properties, including defects and heterogeneity of surface coverage, can result in differences between materials with otherwise identical properties. Generally, covalent functionalization is preferable in order to avoid the loss of surface functionality, although in many cases the as-modified ENM will acquire additional surface coatings that vary with its environment and are often the dominant factor in controlling the biological activity. Control of orientation and distance between the NP and the attached ligand are critical in retaining biomolecule activity, but this has not been fully mastered.

Characterization of nanomaterials is mandatory for their reproducible commercial production and for all applications, including therapeutics, bio-diagnostics, and products that result in close contact between the nanomaterial and the human body (*i.e.* cosmetics, textiles, food). Analytical methods have evolved during the last two decades, with significant advances in sensitivity and ease of use. Despite these technological advances, as reviewed here, many methods are complex, expensive, and require skilled operators. They frequently require detailed knowledge of the principles and, most importantly, the limitations of the method in order to correctly assess specific nanomaterial properties. Furthermore, the quantitative characterization of ENM in biologically-relevant environments, such as blood, cells, and tissues, remains a challenge. The lack of adequate characterization of nanomaterials in relevant environments (whether the human body, consumer products, or the environment) is recognized as a major limitation for the assessment of the effects of ENM

on human health. This problem must be addressed in order to develop realistic and enforceable regulatory requirements for the rapidly expanding nanotechnology field.

For human health applications, there are several challenges that will need to be addressed in the next decade. We can perhaps start with robust, environmentally friendly synthetic procedures that enable the preparation and purification of multifunctional nanoparticles on an industrial scale (*i.e.* to fulfil the vision of theranostics or multimodal therapies). Specific to antibody-coated nanomaterials, the future trends will likely be directed towards replacing the antibodies as the recognition elements by imprinting or engineering their binding epitopes directly to the NP surface (*i.e.* plastic antibodies). This would mitigate problems related to the loss of antibody activity due to denaturation or incorrect orientation when adsorbed on the surface and also long-term storage issues of antibody-conjugated NP. The concept of plastic antibodies along with carefully engineered NP surfaces (*e.g.* to protect the load from the environment, control the load release or minimize protein corona effects) could also reduce challenges associated with poor circulation half-life and premature clearing from the body and could even open new possibilities for the development of oral formulations for nanomedicine products. In this regard, it will be critical to measure and understand the changes in properties that occur when nanomedical products are introduced to the 'hostile' environment of the gastrointestinal tract and when (or if) they are metabolized in the liver. It will also be crucial to fully elucidate the formation of a protein corona on nanoparticles in contact with biological systems.

Nanomaterials have been used systematically for decades, and also by chance for centuries, in various products of our daily life. Over the past few decades, we have learned how to manipulate materials on their atomic scale and how to produce totally new nanoscale materials with various novel features and properties. We have undoubtedly entered a new era with vast opportunities where nanotechnology and nanomaterials can be exploited in a huge number of possible applications. Companies and users often begin by considering only the business benefits or the advantages of a new material, but the past has demonstrated that materials and chemicals may have adverse effects for human health or the environment. As this is important for the sustainability and the safety of nanomaterials, we will address this topic extensively in Part II (Engineered Nanomaterials and Human Health: Applications and Nanotoxicology).

Membership of sponsoring bodies

Membership of the Chemistry and Human Health Division during the preparation of this report (2016–2017) was as follows:

President: T. J. Perun (USA); **Vice President:** R. Cornelis (Belgium); **Secretary:** M. Schwenk (Germany); **Titular Members:** V. Abbate (UK), E. Differding (Belgium), L. Johnston (Canada), H. Møller Johannessen (Denmark), V. Gubala (UK), A. Ganesan (UK); **Associate Members:** S. Alihodzic (Croatia), A. Borzacchiello (Italy), Geok Bee Teh (Malaysia), U. Forsum (Sweden), B. Balasubramanian (USA); **National Representatives:** P. Dolashka-Angelova (Bulgaria), R. Jih-Ru Hwu (China/Taipei), M. Kiilunen (Finland), Chulbom Lee (Korea), Bengt Erik Haug (Norway), M. Saeed Iqbal (Pakistan), N. Carballeira (Puerto Rico), S. O. Bachurin (Russia), J. Blackburn (South Africa).

Membership of the Polymer Division during the preparation of this report (2016–2017) was as follows:

President: G. Russell (New Zealand); **Past President:** M. Buback (Germany); **Vice President:** C. Luscombe (USA); **Secretary:** M. Walter (USA); **Titular Members:** S. Beuermann (Germany), Jiasong He (China/Beijing), I. Lacik (Slovakia), M. Sawamoto (Japan), N. Stingelin (UK), Y. Yagci (Turkey); **Associate Members:** R. Hiorns (France), M. Hess (Germany), G. Moad (Australia), R. Hutchinson (Canada), R. Advincula (USA), D. Auhl (Netherlands); **National Representatives:** C. dos Santos (Brazil), Chain-Shu Hsu (China/Taipei), J. Vohlídal (Czech Republic), M. Malinconico (Italy), Doo Sung Lee (Korea), Chin-Han Chan (Malaysia), R. Adhikari (Nepal), O. E. Philippova (Russia), V. Hoven (Thailand), R.G. Jones (UK).

Funding: Funder Name: International Union of Pure and Applied Chemistry, Funder Id: 10.13039/100006987, Grant Number: 2013-007-1-700.

References

[1] C. J. Moore, H. Monton, R. O'Kennedy, D. E. Williams, C. Nogues, C. Crean, V. Gubala. *J. Mater. Chem. B* **3**, 2043 (2015).
[2] B. Song, Y. Zhang, J. Liu, X. Feng, T. Zhou, L. Shao. *Nanoscale Res. Lett.* **11**, 291 (2016).
[3] F. Grande, P. Tucci. *Mini-Rev. Med. Chem.* **16**, 762 (2016).
[4] S. Borowska, M. M. Brzoska. *J. Appl. Toxicol.* **35**, 551 (2015).
[5] M. Notarianni, J. Liu, K. Vernon, N. Motta. *Beilstein J. Nanotechnol.* **7**, 149 (2016)
[6] S. K. Konda, A. Chen. *Mater. Today* **19**, 100 (2016).
[7] M. Ates. *J. Adhes. Sci. Technol.* **30**, 1510 (2016).
[8] A. K. Yetisen, H. Qu, A. Manbachi, H. Butt, M. R. Dokmeci, J. P. Hinestroza, M. Skorobogatiy, A. Khademhosseini, S. H. Yun. *ACS Nano* **10**, 3042 (2016).
[9] R. Podila, J. M. Brown. *J. Biochem. Mol. Toxic.* **27**, 50 (2013).
[10] K. L. Aillon, Y. Xie, N. El-Gendy, C. J. Berkland, M. L. Forrest. *Adv. Drug Deliver. Rev.* **61**, 457 (2009).
[11] S. W. Shin, I. H. Song, S. H. Um. *Nanomater.* **5**, 1351 (2015).
[12] S. L. Harper, J. L. Carriere, J. M. Miller, J. E. Hutchison, B. L. S. Maddux, R. L. Tanguay. *ACS Nano* **5**, 4688 (2011).
[13] M. E. Vance, T. Kuiken, E. P. Vejerano, S. P. McGinnis, M. F. Hochella, Jr., D. Rejeski, M. S. Hull. *Beilstein J. Nanotechnol.* **6**, 1769 (2015).
[14] P. Evers. In Nanotechnology in Medical Applications: The Global Market. BCC Research, HLC069C (2015).
[15] D. R. Boverhof, C. M. Bramante, J. H. Butala, S. F. Clancy, M. Lafranconi, J. West, S. C. Gordon. *Regul. Toxicol. Pharm.* **73**, 137 (2015).
[16] CODATA-VAMAS Working Group on the Description of Nanomaterials Uniform Descriptor System for Materials on the Nanoscale, version 1.0 (2015).
[17] ISO/TC 229/JWG 1, Nanotechnologies, Terminology and Nomenclature (2005).
[18] European Commission, Commission Recommendation of 18 October 2011 on the definition of nanomaterial (2011).
[19] ISO 80004-1, Nanotechnologies, Vocabulary, Part 1: Core terms (2010).
[20] ISO 80004-2, Nanotechnologies, Vocabulary, Part 2: Nano-objects (2015).
[21] M. Vert, Y. Doi, K.-H. Hellwich, M. Hess, P. Hodge, P. Kubisa, M. Rinaudo, F. Schué. *Pure Appl. Chem.* **84**, 377 (2012).
[22] H. F. Krug, P. Wick. *Angew. Chem. Int. Ed.* **50**, 1260 (2011).
[23] J. A. Lee, M. K. Kim, J. H. Song, M. R. Jo, J. Yu, K. M. Kim, Y. R. Kim, J. M. Oh, S. J. Choi. *Colloids Surf. B Biointerfaces* **150**, 384 (2017).
[24] G. Canché-Escamilla, S. Duarte-Aranda, M. Toledano. *Mater. Sci. Eng. C* **42**, 161 (2014).
[25] I. A. Rahman, V. Padavettan. *J. Nanomater.* **2012**, 8 (2012).
[26] W. Stöber, A. Fink, E. Bohn. *J. Colloid Interf. Sci.* **26**, 62 (1968).
[27] X.-D. Wang, Z.-X. Shen, T. Sang, X.-B. Cheng, M.-F. Li, L.-Y. Chen, Z.-S. Wang. *J. Colloid Interf. Sci.* **341**, 23 (2010).
[28] I. Rahman, P. Vejayakumaran, C. Sipaut, J. Ismail, M. A. Bakar, R. Adnan, C. Chee. *Colloid. Surface. A* **294**, 102 (2007).
[29] Z. X. Li, J. C. Barnes, A. Bosoy, J. F. Stoddart, J. I. Zink. *Chem. Soc. Rev.* **41**, 2590 (2012).
[30] P. P. Yang, S. L. Gai, J. Lin. *Chem. Soc. Rev.* **41**, 3679 (2012).
[31] I. Rahman, P. Vejayakumaran, C. Sipaut, J. Ismail, M. A. Bakar, R. Adnan, C. Chee. *Ceram. Int.* **32**, 691 (2006).
[32] R. I. Nooney, D. Thirunavukkarasu, Y. Chen, R. Josephs, A. E. Ostafin. *Chem. Mater.* **14**, 4721 (2002).
[33] F. Tang, L. Li, D. Chen. *Adv. Mater.* **24**, 1504 (2012).
[34] B. G. Trewyn, I. I. Slowing, S. Giri, H.-T. Chen, V. S.-Y. Lin. *Acc. Chem. Res.* **40**, 846 (2007).
[35] I. I. Slowing, J. L. Vivero-Escoto, B. G. Trewyn, V. S.-Y. Lin. *J. Mater. Chem.* **20**, 7924 (2010).
[36] K. Ma, H. Sai, U. Wiesner. *J. Am. Chem. Soc.* **134**, 13180 (2012).
[37] K. Ma, C. Mendoza, M. Hanson, U. Werner-Zwanziger, J. Zwanziger, U. Wiesner. *Chem. Mater.* **27**, 4119 (2015).
[38] N. Rahimi, R. A. Pax, E. M. Gray. *Prog. Solid State Chem.* **44**, 86 (2016).
[39] Z. A. Lewicka, A. F. Benedetto, D. N. Benoit, W. Y. William, J. D. Fortner, V. L. Colvin. *J. Nanopart. Res.* **13**, 3607 (2011).
[40] Y. Yang, K. Doudrick, X. Y. Bi, K. Hristovski, P. Herckes, P. Westerhoff, R. Kaegi. *Environ. Sci. Technol.* **48**, 6391 (2014).
[41] R. C. Mehrotra, A. Singh. *Chem. Soc. Rev.* **25**, 1 (1996).
[42] P. Arnal, R. J. Corriu, D. Leclercq, P. H. Mutin, A. Vioux. *Chem. Mater.* **9**, 694 (1997).
[43] M. Cargnello, T. R. Gordon, C. B. Murray. *Chem. Rev.* **114**, 9319 (2014).
[44] X. Chen, S. S. Mao. *Chem. Rev.* **107**, 2891 (2007).
[45] B. Tian, F. Chen, J. Zhang, M. Anpo. *J. Colloid Interf. Sci.* **303**, 142 (2006).
[46] A. Chemseddine, T. Moritz. *Eur. J. Inorg. Chem.* **1999**, 235 (1999).
[47] S. Han, S. H. Choi, S. S. Kim, M. Cho, B. Jang, D. Y. Kim, J. Yoon, T. Hyeon. *Small* **1**, 812 (2005).
[48] K. Do Kim, S. H. Kim, H. T. Kim. *Colloid. Surface. A* **254**, 99 (2005).
[49] K. T. Lim, H. S. Hwang, W. Ryoo, K. P. Johnston. *Langmuir* **20**, 2466 (2004).
[50] D. Zhang, L. Qi, J. Ma, H. Cheng. *J. Mater. Chem.* **12**, 3677 (2002).
[51] J. Lin, Y. Lin, P. Liu, M. J. Meziani, L. F. Allard, Y.-P. Sun. *J. Am. Chem. Soc.* **124**, 11514 (2002).
[52] J. K. Oh, J. M. Park. *Prog. Polym. Sci.* **36**, 168 (2011).

[53] C. Sun, J. S. Lee, M. Zhang. *Adv. Drug Deliv. Rev.* **60**, 1252 (2008).
[54] C. Gruttner, J. Teller, W. Schutt, F. Westphal, C. Schumichen, B. Paulke, U. Häfeli, W. Schütt, J. Teller, M. Zborowski. *Scientific and Clinical Applications of Magnetic Carriers*, Plenum Press, New York (1997).
[55] S. Laurent, D. Forge, M. Port, A. Roch, C. Robic, L. Vander Elst, R. N. Muller. *Chem. Rev.* **108**, 2064 (2008).
[56] Y. Deng, L. Wang, W. Yang, S. Fu, A. Elaıssari. *J. Magn. Magn. Mater.* **257**, 69 (2003).
[57] R. E. Johnsen, K. D. Knudsen, A. M. Molenbroek. *J. Appl. Crystallogr.* **44**, 495 (2011).
[58] R. A. Mukh-Qasem, A. Gedanken. *J. Colloid Interf. Sci.* **284**, 489 (2005).
[59] J. Wan, X. Chen, Z. Wang, X. Yang, Y. Qian. *J. Cryst. Growth* **276**, 571 (2005).
[60] W. Wu, Z. Wu, T. Yu, C. Jiang, W.-S. Kim. *Sci. Technol. Adv. Mater.* **16**, 023501 (2015).
[61] S. Basak, D.-R. Chen, P. Biswas. *Chem. Eng. Sci.* **62**, 1263 (2007).
[62] Y. S. Kang, S. Risbud, J. F. Rabolt, P. Stroeve. *Chem. Mater.* **8**, 2209 (1996).
[63] V. K. LaMer, R. H. Dinegar. *J. Am. Chem. Soc.* **72**, 4847 (1950).
[64] R. Hao, R. Xing, Z. Xu, Y. Hou, S. Gao, S. Sun. *Adv. Mater.* **22**, 2729 (2010).
[65] S. Sun, H. Zeng. *J. Am. Chem. Soc.* **124**, 8204 (2002).
[66] T. Hyeon, S. S. Lee, J. Park, Y. Chung, H. B. Na. *J. Am. Chem. Soc.* **123**, 12798 (2001).
[67] S. Sun, H. Zeng, D. B. Robinson, S. Raoux, P. M. Rice, S. X. Wang, G. Li. *J. Am. Chem. Soc.* **126**, 273 (2004).
[68] A. Hütten, D. Sudfeld, I. Ennen, G. Reiss, K. Wojczykowski, P. Jutzi. *J. Magn. Magn. Mater.* **293**, 93 (2005).
[69] D. L. Huber. *Small* **1**, 482 (2005).
[70] C. T. Seip, C. J. O'Connor. *Nanostruct. Mater.* **12**, 183 (1999).
[71] F. Li, C. Vipulanandan, K. K. Mohanty. *Colloid. Surface. A* **223**, 103 (2003).
[72] A. Martino, M. Stoker, M. Hicks, C. H. Bartholomew, A. G. Sault, J. S. Kawola. *Appl. Catal. A-Gen.* **161**, 235 (1997).
[73] B. Jeyadevan, A. Hobo, K. Urakawa, C. Chinnasamy, K. Shinoda, K. Tohji. *J. Appl. Phys.* **93**, 7574 (2003).
[74] S. Zoriasatain, F. Azarkharman, S. Sebt, M. Akhavan. *J. Magn. Magn. Mater.* **300**, 525 (2006).
[75] J. Huang, L. He, Y. Leng, W. Zhang, X. Li, C. Chen, Y. Liu. *Nanotechnology* **18**, 415603 (2007).
[76] B. L. Cushing, V. L. Kolesnichenko, C. J. O'Connor. *Chem. Rev.* **104**, 3893 (2004).
[77] P. Alexandridis. *Chem. Eng. Technol.* **34**, 15 (2011).
[78] S. T. Selvan, T. T. Y. Tan, D. K. Yi, N. R. Jana. *Langmuir* **26**, 11631 (2009).
[79] L. Y. Chen, C. W. Wang, Z. Yuan, H. T. Chang. *Anal. Chem.* **87**, 216 (2015).
[80] K. Saha, S. S. Agasti, C. Kim, X. Li, V. M. Rotello. *Chem. Rev.* **112**, 2739 (2012).
[81] J. Turkevich, P. C. Stevenson, J. Hillier. *Discuss. Faraday Soc.* **11**, 55 (1951).
[82] M. Brust, M. Walker, D. Bethell, D. J. Schiffrin, R. Whyman. *J. Chem. Soc. Chem. Commun.* **0**, 801 (1994).
[83] T. Sakai, P. Alexandridis. *Langmuir* **20**, 8426 (2004).
[84] C. J. Murphy. *Science* **298**, 2139 (2002).
[85] I. Sondi, B. Salopek-Sondi. *J. Colloid Interf. Sci.* **275**, 177 (2004).
[86] R. B. Reed, T. Zaikova, A. Barber, M. Simonich, R. Lankone, M. Marco, K. Hristovski, P. Herckes, L. Passantino, D. H. Fairbrother, R. Tanguay, J. F. Ranville, J. E. Hutchison, P. K. Westerhoff. *Environ. Sci. Technol.* **50**, 4018 (2016).
[87] D. D. Evanoff, G. Chumanov. *ChemPhysChem* **6**, 1221 (2005).
[88] S. Chernousova, M. Epple. *Angew. Chem. Int. Ed.* **52**, 1636 (2013).
[89] Y. N. Xia, Y. J. Xiong, B. Lim, S. E. Skrabalak. *Angew. Chem. Int. Ed.* **48**, 60 (2009).
[90] F. Mafune, J. Kohno, Y. Takeda, T. Kondow, H. Sawabe. *J. Phys. Chem. B* **104**, 8333 (2000).
[91] J. Neddersen, G. Chumanov, T. M. Cotton. *Appl. Spectrosc.* **47**, 1959 (1993).
[92] S. Zhang, Y. Tang, B. Vlahovic. *Nanosc. Res. Lett.* **11**, 80, 1 (2016).
[93] T. W. Giessen, P. A. Silver. *ACS Synth. Biol.* **16**, 1497 (2016).
[94] M. A. Dar, A. Ingle, M. Rai. *Nanomed. Nanotechnol.* **9**, 105 (2013).
[95] S. P. Chandran, M. Chaudhary, R. Pasricha, A. Ahmad, M. Sastry. *Biotechnol. Progr.* **22**, 577 (2006).
[96] R. R. Naik, S. J. Stringer, G. Agarwal, S. E. Jones, M. O. Stone. *Nature Mater.* **1**, 169 (2002).
[97] J. P. Xie, J. Y. Lee, D. I. C. Wang, Y. P. Ting. *ACS Nano* **1**, 429 (2007).
[98] E. Lee, D. H. Kim, Y. Woo, H. G. Hur, Y. Lim. *Biochem. Biophys. Res. Commun.* **376**, 595 (2008).
[99] J. Yao, M. Yang, Y. Duan. *Chem. Rev.* **114**, 6130 (2014).
[100] X. Ji, F. Peng, Y. Zhong, Y. Su, Y. He. *Colloid. Surface. B* **124**, 132 (2014).
[101] W. K. Leutwyler, S. L. Bürgi, H. Burgl. *Science* **271**, 933 (1996).
[102] I. L. Medintz, H. T. Uyeda, E. R. Goldman, H. Mattoussi. *Nat. Mater.* **4**, 435 (2005).
[103] R. Rossetti, S. Nakahara, L. Brus. *J. Chem. Phys.* **79**, 1086 (1983).
[104] C. Murray, D. J. Norris, M. G. Bawendi. *J. Am. Chem. Soc.* **115**, 8706 (1993).
[105] Z. A. Peng, X. Peng. *J. Am. Chem. Soc.* **123**, 183 (2001).
[106] M. A. Hines, P. Guyot-Sionnest. *J. Phys. Chem. B* **100**, 468 (1996).
[107] Y. Tian, T. Newton, N. A. Kotov, D. M. Guldi, J. H. Fendler. *J. Phys. Chem. B* **100**, 8927 (1996).
[108] H. C. Youn, S. Baral, J. H. Fendler. *J. Phys. Chem.* **92**, 6320 (1988).
[109] B. Dabbousi, J. Rodriguez-Viejo, F. V. Mikulec, J. Heine, H. Mattoussi, R. Ober, K. Jensen, M. Bawendi. *J. Phys. Chem. B* **101**, 9463 (1997).

[110] H. Zhang, L.-p. Wang, H. Xiong, L. Hu, B. Yang, W. Li. *Adv. Mater.* **15**, 1712 (2003).
[111] X. Michalet, F. F. Pinaud, L. A. Bentolila, J. M. Tsay, S. Doose, J. J. Li, G. Sundaresan, A. M. Wu, S. S. Gambhir, S. Weiss. *Science* **307**, 538 (2005).
[112] J. Rockenberger, L. Tröger, A. L. Rogach, M. Tischer, M. Grundmann, A. Eychmüller, H. Weller. *J. Chem. Phys.* **108**, 7807 (1998).
[113] M. Gao, S. Kirstein, H. Möhwald, A. L. Rogach, A. Kornowski, A. Eychmüller, H. Weller. *J. Phys. Chem. B* **102**, 8360 (1998).
[114] N. N. Mamedova, N. A. Kotov, A. L. Rogach, J. Studer. *Nano Lett.* **1**, 281 (2001).
[115] N. Gaponik, D. V. Talapin, A. L. Rogach, K. Hoppe, E. V. Shevchenko, A. Kornowski, A. Eychmüller, H. Weller. *J. Phys. Chem. B* **106**, 7177 (2002).
[116] Y. He, H.-T. Lu, L.-M. Sai, Y.-Y. Su, M. Hu, C.-H. Fan, W. Huang, L.-H. Wang. *Adv. Mater* **20**, 3416 (2008).
[117] H. Qian, X. Qiu, L. Li, J. Ren. *J. Phys. Chem. B* **110**, 9034 (2006).
[118] L. Li, H. Qian, J. Ren. *Chem. Commun.* **0**, 528 (2005).
[119] N. Kamaly, Z. Xiao, P. M. Valencia, A. F. Radovic-Moreno, O. C. Farokhzad. *Chem. Soc. Rev.* **41**, 2971 (2012).
[120] M. E. Caldorera-Moore, W. B. Liechty, N. A. Peppas. *Acc. Chem. Res.* **44**, 1061 (2011).
[121] R. Langer, J. Folkman. *Nature* **263**, 797 (1976).
[122] O. C. Farokhzad, R. Langer. *Adv. Drug Deliv. Rev.* **58**, 1456 (2006).
[123] A. Kumari, S. K. Yadav, S. C. Yadav. *Colloid. Surface. B* **75**, 1 (2010).
[124] F. Danhier, E. Ansorena, J. M. Silva, R. Coco, A. Le Breton, V. Préat. *J. Control. Release* **161**, 505 (2012).
[125] H.-Y. Kwon, J.-Y. Lee, S.-W. Choi, Y. Jang, J.-H. Kim. *Colloid. Surface. A* **182**, 123 (2001).
[126] P. Ahlin Grabnar, J. Kristl. *J. Microencapsul.* **28**, 323 (2011).
[127] M. Zambaux, F. Bonneaux, R. Gref, E. Dellacherie, C. Vigneron. *J. Control. Release* **60**, 179 (1999).
[128] M. Hans, A. Lowman. *Curr. Opin. Solid State Mater. Sci.* **6**, 319 (2002).
[129] K. S. Soppimath, T. M. Aminabhavi, A. R. Kulkarni, W. E. Rudzinski. *J. Control. Release* **70**, 1 (2001).
[130] P. Couvreur, B. Kante, M. Roland, P. Guiot, P. Bauduin, P. Speiser. *J. Pharm. Pharmacol.* **31**, 331 (1979).
[131] H. Fessi, F. Puisieux, J. P. Devissaguet, N. Ammoury, S. Benita. *Int. J. Pharm.* **55**, R1 (1989).
[132] T. Jung, W. Kamm, A. Breitenbach, E. Kaiserling, J. Xiao, T. Kissel. *Eur. J. Pharm. Biopharm.* **50**, 147 (2000).
[133] C. P. Reis, R. J. Neufeld, A. J. Ribeiro, F. Veiga. *Nanomed. Nanotech. Biol. Med.* **2**, 8 (2006).
[134] E. Allémann, J.-C. Leroux, R. Gurny, E. Doelker. *Pharm. Res.* **10**, 1732 (1993).
[135] M. Vert. *Int. J. Artif. Organs* **34**, 76 (2011).
[136] N. Anton, J.-P. Benoit, P. Saulnier. *J. Control. Release* **128**, 185 (2008).
[137] K. Avgoustakis. *Curr. Drug Deliv.* **1**, 321 (2004).
[138] T. R. Tice, R. M. Gilley. *J. Control. Release* **2**, 343 (1985)
[139] J. M. Barichello, M. Morishita, K. Takayama, T. Nagai. *Drug Dev. Ind. Pharm.* **25**, 471 (1999).
[140] S. Galindo-Rodriguez, E. Allemann, H. Fessi, E. Doelker. *Pharm. Res.* **21**, 1428 (2004).
[141] F. Ganachaud, J. L. Katz. *ChemPhysChem* **6**, 209 (2005).
[142] D. Quintanar-Guerrero, E. Allémann, H. Fessi, E. Doelker. *Drug Dev. Ind. Pharm.* **24**, 1113 (1998).
[143] A. Avital, E. Shapiro, V. Doviner, Y. Sherman, S. Margel, M. Tsuberi, C. Springer. *Am. J. Respir. Cell Mol. Biol.* **27**, 511 (2002).
[144] K. Tauer, R. Deckwer, I. Kühn, C. Schellenberg. *Colloid. Polym. Sci.* **277**, 607 (1999).
[145] S. Hornig, T. Heinze, C. R. Becer, U. S. Schubert. *J. Mater. Chem.* **19**, 3838 (2009).
[146] N. Miletić, V. Abetz, K. Ebert, K. Loos. *Macromol. Rapid Commun.* **31**, 71 (2010).
[147] Y. Li, H. Dong, K. Wang, D. Shi, X. Zhang, R. Zhuo. *Sci. China Chem.* **53**, 447 (2010).
[148] S. Kim, C.-K. Lim, J. Na, Y.-D. Lee, K. Kim, K. Choi, J. F. Leary, I. C. Kwon. *Chem. Commun.* **46**, 1617 (2010).
[149] L. Radushkevich, V. Lukyanovich. *Zurn. Fisic. Chim.* **26**, 88 (1952).
[150] S. Iijima. *Nature* **354**, 56 (1991).
[151] S. Vardharajula, S. Z. Ali, P. M. Tiwari, E. Eroğlu, K. Vig, V. A. Dennis, S. R. Singh. *Int. J. Nanomed.* **7**, 5361 (2012).
[152] A. Szabó, C. Perri, A. Csató, G. Giordano, D. Vuono, J. B. Nagy. *Materials* **3**, 3092 (2010).
[153] T. Guo, P. Nikolaev, A. Thess, D. Colbert, R. Smalley. *Chem. Phys. Lett.* **243**, 49 (1995).
[154] N. Braidy, M. El Khakani, G. Botton. *Carbon* **40**, 2835 (2002).
[155] J. W. Seo, A. Magrez, M. Milas, K. Lee, V. Lukovac, L. Forró. *J. Phys. D Appl. Phys.* **40**, R109 (2007).
[156] P.-X. Hou, C. Liu, H.-M. Cheng. *Carbon* **46**, 2003 (2008).
[157] S. Kawasaki, M. Shinoda, T. Shimada, F. Okino, H. Touhara. *Carbon* **44**, 2139 (2006).
[158] A. D. Bangham, M. M. Standish, J. C. Watkins. *J. Mol. Biol.* **13**, 238 (1965).
[159] P. P. Deshpande, S. Biswas, V. P. Torchilin. *Nanomedicine* **8**, 1509 (2013).
[160] H.-I. Chang, M.-K. Yeh. *Int. J. Nanomed.* **7**, 49 (2012).
[161] T. M. Allen, P. R. Cullis. *Adv. Drug Deliv. Rev.* **65**, 36 (2013).
[162] Z. Cheng, A. Al Zaki, J. Z. Hui, V. R. Muzykantov, A. Tsourkas. *Science* **338**, 903 (2012).
[163] M. D. Moen, K. A. Lyseng-Williamson, L. J. Scott. *Drugs* **69**, 361 (2009).
[164] W. Lohcharoenkal, L. Wang, Y. C. Chen, Y. Rojanasakul. *BioMed Res. Int.* **2014**, 1 (2014).
[165] D. He, J. Marles-Wright. *New Biotechnol.* **32**, 651 (2015).
[166] J. López-Sagaseta, E. Malito, R. Rappuoli, M. J. Bottomley. *Comput. Struct. Biotechnol. J.* **14**, 58 (2016).

[167] V. Kumar, S. Palazzolo, S. Bayda, G. Corona, G. Toffoli, F. Rizzolio. *Theranostics* **6**, 710 (2016).
[168] J. J. Rossi. *Acta Biochim. Biophys. Sin.* **43**, 245 (2011).
[169] N. Erathodiyil, J. Y. Ying. *Acc. Chem. Res.* **44**, 925 (2011).
[170] R. Mout, D. F. Moyano, S. Rana, V. M. Rotello. *Chem. Soc. Rev.* **41**, 2539 (2012).
[171] C. Steinbach. *Coatings for Nanomaterials*. DECHEMA e.V., Frankfurt a. M. (2014).
[172] R. A. Sperling, W. J. Parak. *Ther. Innov. Regul. Sci.* **47**, 1333 (2013).
[173] A. Sedlmeier, H. H. Gorris. *Chem. Soc. Rev.* **44**, 1526 (2015).
[174] S. K. Natarajan, S. Selvaraj. *RSC Adv.* **4**, 14328 (2014).
[175] M. Muthiah, I.-K. Park, C.-S. Cho. *Biotechnol. Adv.* **31**, 1224 (2013).
[176] D. Ling, M. J. Hackett, T. Hyeon. *Nano Today* **9**, 457 (2014).
[177] K. E. Sapsford, W. R. Algar, L. Berti, K. B. Gemmill, B. J. Casey, E. Oh, M. H. Stewart, I. L. Medintz. *Chem. Rev.* **113**, 1904 (2013).
[178] B. Saha, T. H. Evers, M. W. J. Prins. *Anal. Chem.* **86**, 8158 (2014).
[179] M. P. Monopoli, C. Aberg, A. Salvati, K. A. Dawson. *Nature Nanotechnol.* **7**, 779 (2012).
[180] A. Schroedter, H. Weller. *Angew. Chem. Int. Ed.* **41**, 3218 (2002).
[181] Z. Zhelev, H. Ohba, R. Bakalova. *J. Am. Chem. Soc.* **128**, 6324 (2006).
[182] D. Giaume, M. Poggi, D. Casanova, G. Mialon, K. Lahlil, A. Alexandrou, T. Gacoin, J.-P. Boilot. *Langmuir* **24**, 11018 (2008).
[183] S. Santra, H. Yang, P. H. Holloway, J. T. Stanley, R. A. Mericle. *J. Am. Chem. Soc.* **127**, 1656 (2005).
[184] E. P. Plueddemann, H. Clark, L. Nelson, K. Hoffman. *Modern Plastics* **39**, 135 (1962).
[185] M. Ohmori, E. Matijević. *J. Colloid Interf. Sci.* **160**, 288 (1993).
[186] L. M. Liz-Marzán, A. P. Philipse. *J. Colloid Interf. Sci.* **176**, 459 (1995).
[187] M. Li, H. Schnablegger, S. Mann. *Nature* **402**, 393 (1999).
[188] J. N. Liu, W. B. Bu, J. L. Shi. *Acc. Chem. Res.* **48**, 1797 (2015).
[189] P. D. I. Fletcher, B. Holt. *Langmuir* **27**, 12869 (2011).
[190] Y. Liu, Y. M. Li, X. M. Li, T. He. *Langmuir* **29**, 15275 (2013).
[191] A. Schoth, A. D. Keith, K. Landfester, R. Munoz-Espi. *RSC Adv.* **6**, 53903 (2016).
[192] E. Tang, H. Liu, L. Sun, E. Zheng, G. Cheng. *Eur. Polym. J.* **43**, 4210 (2007).
[193] E. Ukaji, T. Furusawa, M. Sato, N. Suzuki. *Appl. Surf. Sci.* **254**, 563 (2007).
[194] J. Zhao, M. Milanova, M. M. Warmoeskerken, V. Dutschk. *Colloids Surf. A* **413**, 273 (2012).
[195] Y. Guo, M. Wang, H. Zhang, G. Liu, L. Zhang, X. Qu. *J. Appl. Polym. Sci.* **107**, 2671 (2008).
[196] L. M. Liz-Marzán, M. Giersig, P. Mulvaney. *Langmuir* **12**, 4329 (1996).
[197] C. Graf, D. L. Vossen, A. Imhof, A. van Blaaderen. *Langmuir* **19**, 6693 (2003).
[198] M. Chen, L. Wu, S. Zhou, B. You. *Adv. Mater.* **18**, 801 (2006).
[199] Y. Yang, L. Jing, X. Yu, D. Yan, M. Gao. *Chem. Mater.* **19**, 4123 (2007).
[200] R. Koole, M. M. van Schooneveld, J. Hilhorst, C. de Mello Donegá, D. C. 't. Hart, A. van Blaaderen, D. Vanmaekelbergh, A. Meijerink. *Chem. Mater.* **20**, 2503 (2008).
[201] M. Darbandi, R. Thomann, T. Nann. *Chem. Mater.* **17**, 5720 (2005).
[202] J. Nam, N. Won, J. Bang, H. Jin, J. Park, S. Jung, S. Jung, Y. Park, S. Kim. *Adv. Drug Deliv. Rev.* **65**, 622 (2013).
[203] T. Pellegrino, L. Manna, S. Kudera, T. Liedl, D. Koktysh, A. L. Rogach, S. Keller, J. Rädler, G. Natile, W. J. Parak. *Nano Lett.* **4**, 703 (2004).
[204] M. A. White, J. A. Johnson, J. T. Koberstein, N. J. Turro. *J. Am. Chem. Soc.* **128**, 11356 (2006).
[205] H. Mattoussi, J. M. Mauro, E. R. Goldman, G. P. Anderson, V. C. Sundar, F. V. Mikulec, M. G. Bawendi. *JACS* **122**, 12142 (2000).
[206] W. Liu, M. Howarth, A. B. Greytak, Y. Zheng, D. G. Nocera, A. Y. Ting, M. G. Bawendi. *J. Am. Chem. Soc.* **130**, 1274 (2008).
[207] F. Dubois, B. Mahler, B. Dubertret, E. Doris, C. Mioskowski. *J. Am. Chem. Soc.* **129**, 482 (2007).
[208] W. C. Chan, S. Nie. *Science* **281**, 2016 (1998).
[209] H. Jin, J. Nam, J. Park, S. Jung, K. Im, J. Hur, J.-J. Park, J.-M. Kim, S. Kim. *Chem. Commun.* **47**, 1758 (2011).
[210] A. Swami, A. Kumar, M. Sastry. *Langmuir* **19**, 1168 (2003).
[211] D. E. Owens, N. A. Peppas. *Int. J. Pharm.* **307**, 93 (2006).
[212] K. G. Neoh, E. T. Kang. *Polym. Chem.* **2**, 747 (2011).
[213] B. Pelaz, P. del Pino, P. Maffre, R. Hartmann, M. Gallego, S. Rivera-Fernandez, J. M. de la Fuente, G. U. Nienhaus, W. J. Parak. *ACS Nano* **9**, 6996 (2015).
[214] J. Virkutyte, R. S. Varma. *Chem. Sci.* **2**, 837 (2011).
[215] L. E. van Vlerken, T. K. Vyas, M. M. Amiji. *Pharm. Res.* **24**, 1405 (2007).
[216] J. Chen, S. K. Spear, J. G. Huddleston, R. D. Rogers. *Green Chem.* **7**, 64 (2005).
[217] A. S. Karakoti, S. Das, S. Thevuthasan, S. Seal. *Angew. Chem. Int. Ed.* **50**, 1980 (2011).
[218] Z. P. Xu, Q. H. Zeng, G. Q. Lu, A. B. Yu. *Chem. Eng. Sci.* **61**, 1027 (2006).
[219] M. D. Howard, M. Jay, T. D. Dziubla, X. Lu. *J. Biomed. Nanotechnol.* **4**, 133 (2008).
[220] C.-J. Liu, C.-H. Wang, S.-T. Chen, H.-H. Chen, W.-H. Leng, C.-C. Chien, C.-L. Wang, I. M. Kempson, Y. Hwu, T.-C. Lai. *Phys. Med. Biol.* **55**, 931 (2010).

[221] G. Zhang, Z. Yang, W. Lu, R. Zhang, Q. Huang, M. Tian, L. Li, D. Liang, C. Li. *Biomater.* **30**, 1928 (2009).
[222] J. Gao, X. Huang, H. Liu, F. Zan, J. Ren. *Langmuir* **28**, 4464 (2012).
[223] E. K. Larsen, T. Nielsen, T. Wittenborn, H. Birkedal, T. Vorup-Jensen, M. H. Jakobsen, L. Østergaard, M. R. Horsman, F. Besenbacher, K. A. Howard. *ACS Nano* **3**, 1947 (2009).
[224] S. Wan, J. Huang, H. Yan, K. Liu. *J. Mater. Chem.* **16**, 298 (2006).
[225] E. Amstad, S. Zurcher, A. Mashaghi, J. Y. Wong, M. Textor, E. Reimhult. *Small* **5**, 1334 (2009).
[226] Z. Li, L. Wei, M. Gao, H. Lei. *Adv. Mater.* **17**, 1001 (2005).
[227] K. Christodoulakis, D. Palioura, S. Anastasiadis, M. Vamvakaki. *Top. Catal.* **52**, 394 (2009).
[228] S. Dunn, S. Stolnick, M. Garnett, M. Davies, A. Coombes, D. Taylor, M. Irving, S. Purkiss, T. F. Tadros, S. Davis. *Proc. Int. Symp. Controll. Release Bioact. Mater., Control. Release Soc.* **21**, 210 (1994).
[229] B. Müller, T. Kissel. *Pharm. Pharmacol. Lett.* **3**, 67 (1993).
[230] R. Gref, A. Domb, P. Quellec, T. Blunk, R. Müller, J. Verbavatz, R. Langer. *Adv. Drug Deliv. Rev.* **64**, 316 (2012).
[231] M. Vert, D. Domurado. *J. Biomater. Sci. Polym. Ed.* **11**, 1307 (2000).
[232] L. Leclercq, E. Modena, M. Vert. *J. Biomater. Sci. Polym. Ed.* **24**, 1499 (2013).
[233] L. Yan, F. Zhao, S. Li, Z. Hu, Y. Zhao. *Nanoscale* **3**, 362 (2011).
[234] A. A. Bhirde, S. Patel, A. A. Sousa, V. Patel, A. A. Molinolo, Y. Ji, R. D. Leapman, J. S. Gutkind, J. F. Rusling. *Nanomedicine* **5**, 1535 (2010).
[235] H.-F. Cui, S. K. Vashist, K. Al-Rubeaan, J. H. Luong, F.-S. Sheu. *Chem. Res. Toxicol.* **23**, 1131 (2010).
[236] M. Uo, T. Akasaka, F. Watari, Y. Sato, K. Tohji. *Dent. Mater. J.* **30**, 245 (2011).
[237] A. Hirsch, O. Vostrowsky. "Functionalization of carbon nanotubes", in *Functional Molecular Nanostructures*, A. Dieter Schlüter (Ed.), pp. 193–237, Springer, Heidelberg (2005).
[238] Y.-L. Zhao, J. F. Stoddart. *Acc. Chem. Res.* **42**, 1161 (2009).
[239] A. Rinzler, J. Liu, H. Dai, P. Nikolaev, C. Huffman, F. Rodriguez-Macias, P. Boul, A. H. Lu, D. Heymann, D. Colbert. *Appl. Phys. A* **67**, 29 (1998).
[240] E. Dujardin, T. W. Ebbesen, A. Krishnan, M. M. Treacy. *Adv. Mater.* **10**, 611 (1998).
[241] S. Nagasawa, M. Yudasaka, K. Hirahara, T. Ichihashi, S. Iijima. *Chem. Phys. Lett.* **328**, 374 (2000).
[242] G. Sumanasekera, J. Allen, S. Fang, A. Loper, A. Rao, P. Eklund. *J. Phys. Chem. B* **103**, 4292 (1999).
[243] J. Liu, A. G. Rinzler, H. Dai, J. H. Hafner, R. K. Bradley, P. J. Boul, A. Lu, T. Iverson, K. Shelimov, C. B. Huffman. *Science* **280**, 1253 (1998).
[244] K. Morishita, T. Takarada. *J. Mater. Sci.* **34**, 1169 (1999).
[245] T. Goto, H. Takahashi, Y. Shinoda, N. Shimizu, B. Jeyadevan, I. Matsuoka, Y. Saito, A. Kasuya. *Nature* **383**, 679 (1996).
[246] S. Mallakpour, S. Soltanian. *RSC Adv.* **6**, 109916 (2016).
[247] R. J. Chen, Y. Zhang, D. Wang, H. Dai. *J. Am. Chem. Soc.* **123**, 3838 (2001).
[248] M. Melchionna, M. Prato. *ECS J. Solid State Sci. Technol.* **2**, M3040 (2013).
[249] M. Shim, N. W. S. Kam, R. J. Chen, Y. M. Li, H. J. Dai. *Nano Lett.* **2**, 285 (2002).
[250] L. W. Zhang, L. Zeng, A. R. Barron, N. A. Monteiro-Riviere. *Int. J. Toxicol.* **26**, 103 (2007).
[251] N. Nakayama-Ratchford, S. Bangsaruntip, X. Sun, K. Welsher, H. Dai. *J. Am. Chem. Soc.* **129**, 2448 (2007).
[252] M. J. O'Connell, P. Boul, L. M. Ericson, C. Huffman, Y. Wang, E. Haroz, C. Kuper, J. Tour, K. D. Ausman, R. E. Smalley. *Chem. Phys. Lett.* **342**, 265 (2001).
[253] X. Zhang, T. Liu, T. Sreekumar, S. Kumar, V. C. Moore, R. H. Hauge, R. E. Smalley. *Nano Lett.* **3**, 1285 (2003).
[254] R. J. Chen, S. Bangsaruntip, K. A. Drouvalakis, N. W. S. Kam, M. Shim, Y. Li, W. Kim, P. J. Utz, H. Dai. *Proc. Nat. Acad. Sci.* **100**, 4984 (2003).
[255] R. P. Gandhiraman, C. Volcke, V. Gubala, C. Doyle, L. Basabe-Desmonts, C. Dotzler, M. F. Toney, M. Iacono, R. I. Nooney, S. Daniels, B. James, D. E. Williams. *J. Mater. Chem.* **20**, 4116 (2010).
[256] R. P. Gandhiraman, V. Gubala, C. C. O'Mahony, T. Cummins, J. Raj, A. Eltayeb, C. Doyle, B. James, S. Daniels, D. E. Williams. *Vacuum* **86**, 547 (2012).
[257] S. Q. Hutsell, R. J. Kimple, D. P. Siderovski, F. S. Willard, A. J. Kimple. "High-affinity immobilization of proteins using biotin- and GST-based coupling strategies", in *Surf. Plasmon Reson.*, N. J. Mol, M. J. E. Fischer (Eds.), pp. 75–90, Springer Link, Humana Press (2010).
[258] B. Lu, M. R. Smyth, R. OKennedy. *Analyst* **121**, R29 (1996).
[259] J. Turkova. *J. Chromatogr. B* **722**, 11 (1999).
[260] R. P. Ekins. *Clin. Chem.* **44**, 2015 (1998).
[261] F. Rusmini, Z. Y. Zhong, J. Feijen. *Biomacromolecules* **8**, 1775 (2007).
[262] J. V. Jokerst, A. Raamanathan, N. Christodoulides, P. N. Floriano, A. A. Pollard, G. W. Simmons, J. Wong, C. Gage, W. B. Furmaga, S. W. Redding, J. T. McDevitt. *Biosens. Bioelectron.* **24**, 3622 (2009).
[263] P. Jonkheijm, D. Weinrich, H. Schroder, C. M. Niemeyer, H. Waldmann. *Angew. Chem.* **47**, 9618 (2008).
[264] M. Kohn. *J. Pept. Sci.* **15**, 393 (2009).
[265] D. S. Y. Yeo, R. C. Panicker, L. P. Tan, S. Q. Yao. *Comb. Chem. High Throughput Screen.* **7**, 213 (2004).
[266] J. L. Fu, J. Reinhold, N. W. Woodbury. *PLoS One* **6**, e18692 (2011).
[267] V. Gubala, L. F. Harris, A. J. Ricco, M. X. Tan, D. E. Williams. *Anal. Chem.* **84**, 487 (2012).

[268] M. Montalti, L. Prodi, E. Rampazzo, N. Zaccheroni. *Chem. Soc. Rev.* **43**, 4243 (2014).
[269] N. Kaur, K. Subramani, Y. Pathak. "Methods for polymeric nanoparticle conjugation to monoclonal antibodies", in *Antibody-Mediated Drug Delivery Systems*, Y. Pathak, S. Benita (Eds.), pp. 1–12, John Wiley & Sons, Inc., New Jersey (2012).
[270] V. Gubala, X. Le Guevel, R. Nooney, D. E. Williams, B. MacCraith. *Talanta* **81**, 1833 (2010).
[271] G. T. Hermanson. *Bioconjugate Techniques,* 2nd Edition, Academic Press, Rockford, IL, USA (2008).
[272] H. H. Yang, H. Y. Qu, P. Lin, S. H. Li, M. T. Ding, J. G. Xu. *Analyst* **128**, 462 (2003).
[273] S. R. Corrie, G. A. Lawrie, M. Trau. *Langmuir* **22**, 2731 (2006).
[274] M. Qhobosheane, S. Santra, P. Zhang, W. H. Tan. *Analyst* **126**, 1274 (2001).
[275] W. Lian, S. A. Litherland, H. Badrane, W. H. Tan, D. H. Wu, H. V. Baker, P. A. Gulig, D. V. Lim, S. G. Jin. *Anal. Biochem.* **334**, 135 (2004).
[276] V. Gubala, C. Crean, R. Nooney, S. Hearty, B. McDonnell, K. Heydon, R. O'Kennedy, B. D. MacCraith, D. E. Williams. *Analyst* **136**, 2533 (2011).
[277] F. Liu, L. Wang, H. Wang, L. Yuan, J. Li, J. L. Brash, H. Chen. *ACS Appl. Mater. Interfaces* **7**, 3717 (2015).
[278] M. Auffan, J. Rose, J.-Y. Bottero, G. V. Lowry, J.-P. Jolivet, M. R. Wiesner. *Nat. Nanotech.* **4**, 634 (2009).
[279] M. L. Etheridge, S. A. Campbell, A. G. Erdman, C. L. Haynes, S. M. Wolf, J. McCullough. *Nanomedicine* **9**, 1 (2013).
[280] A. G. Oomen, E. A. J. Bleeker, P. M. J. Bos, F. van Broekhuizen, S. Gottardo, M. Groenewold, D. Hristozov, K. Hund-Rinke, M.-A. Irfan, A. Marcomini, W. J. G. M. Peijnenburg, K. Rasmussen, A. S. Jimenez, J. J. Scott-Fordsmand, M. van Tongeren, K. Wiench, W. Wohlleben, R. Landsiedel. *Int. J. Environ. Res. Publ. Health.* **12**, 13415 (2015).
[281] A. B. Stefaniak, V. A. Hackley, G. Roebben, K. Ehara, S. Hankin, M. T. Postek, I. Lynch, W.-E. Fu, T. P. J. Linsinger, A. F. Thunemann. *Nanotoxicol.* **7**, 1325 (2013).
[282] H. F. Krug, P. Wick. *Angew. Chem. Int. Ed.* **50**, 1260 (2011).
[283] H. Bouwmeester, I. Lynch, H. J. P. Marvin, K. A. Dawson, M. Berges, D. Braguer, H. J. Byrne, A. Casey, G. Chambers, M. J. D. Clift, G. Elia, T. F. Fernandes, L. B. Fjellsbo, P. Hatto, L. Juillerat, C. Klein, W. G. Kreyling, C. Nickel, M. Riediker, V. Stone. *Nanotoxicology* **5**, 1 (2011).
[284] D. R. Baer, M. H. Engelhard, G. E. Johnson, J. Laskin, J. Lai, K. Mueller, P. Munusamy, S. Thevuthasan, H. Wang, N. Washton, A. Elder, B. L. Baisch, A. Karakoti, S. V. N. T. Kuchibhatia, D. Moon. *J. Vac. Sci. Technol.* **31**, 050820-050821-050834 (2013).
[285] M. Baalousha, J. R. Lead. *Envir. Sci. Tech.* **46**, 6134 (2012).
[286] N. C. Bell, C. Minelli, J. Tompkins, M. M. Stevens, A. G. Shard. *Langmuir* **28**, 10860 (2012).
[287] S. Smulders, J. P. Kaiser, S. Zuin, K. L. V. Landuyt, L. Golanski, J. Vanoirbeek, P. Wick, P. H. M. Hoet. *Part. Fibre Toxicol.* **9**, 41 (2012).
[288] B. W. Neun, M. A. Dobrovolskaia. *Methods Mol. Biol.* **697**, 121 (2011).
[289] S. J. L. Billinge, I. Levin. *Science* **316**, 561 (2007).
[290] S. C. Brown, V. Boyko, G. Meyers, M. Voetz, W. Wohlleben. *Envir. Health Perspec.* **1221**, 1282 (2013).
[291] T. Linsinger, G. Roebben, D. Gilliland, L. Calzolai, F. Rossi, P. Gibson, Ch. Klein. Publications Office of the European Union, JRC73260, Requirements on measurements for the implementation of the European Commission definition of the term "nanomaterial" (2012)
[292] ASTM E2859-11, Size Measurement of Nanoparticles Using Atomic Force Microscopy (2012).
[293] J. Grobelny, F. W. DelRio, N. Pradeep, D.-I. Kim, V. A. Hackley, R. F. Cook. *National Institute of Standards and Technology and Nanotechnology Characterization Laboratory* **Ver. 1.1** (2009).
[294] F. Meli, T. Klein, E. Buhr, C. G. Frase, G. Gleber, M. Krumrey, A. Duta, S. Duta, V. Korpelainen, R. Bellotti, G. B. Picotto, R. D. Boyd, A. Cuenat. *Meas. Sci. Tech.* **23**, 125005 (2012).
[295] Y. Sun, Y. Xia. *Science* **298**, 2176 (2002).
[296] H. Chen, X. Kou, Z. Yang, W. Ni, J. Wang. *Langmuir* **24**, 5233 (2008).
[297] A. S. Zhao, S. Zhou, Y. Wang, J. Chen, C. R. Ye, N. Huang. *RSC Adv.* **4**, 40428 (2014).
[298] R. Weissleder, M. Nahrendorf, M. J. Pittet. *Nature Mater.* **13**, 125 (2014).
[299] D. Vobornik, S. Zou, G. P. Lopinski. *Langmuir* **32**, 8735 (2016).
[300] ISO/TR 14187, Surface chemical analysis – characterization of nanostructured materials (2011)
[301] ISO 9276-6, Representation of results of particle size analysis – Part 6: Descriptive and quantitative representation of particle shape and morphology (2008).
[302] ISO 13322-1, Particle size analysis – image analysis methods – Part 1: Static image analysis methods (2004).
[303] ISO 14488, Particulate materials – sampling and sample splitting for the determination of particulate properties (2007).
[304] ASTM E2834-12, Standard Guide for Measurement of Particle Size Distribution of Nanomaterials in Suspension by Nanoparticle Tracking Analysis (2012)
[305] ISO 22412, Particle size analysis – dynamic light scattering (2008).
[306] V. Filipe, A. Hawe, W. Jiskoot. *Pharm. Res.* **27**, 796 (2010).
[307] D. Kozaka, W. Anderson, R. Vogel, M. Trau. *Nano Today* **6**, 531 (2011).
[308] ASTM E2490-09, Standard Guide for Measurement of Particle Size Distribution of Nanomaterials in Suspension by Photon Correlation Spectroscopy (2009).

[309] P. Bru, L. Brunel, H. Buron, I. Cayre, X. Ducarre, A. Fraux, O. Mengual, G. Meunier, A. D. S. Marie, P. Snabre. "Particle size and rapid stability analyses of concentrated dispersions", in *Particle Sizing and Characterization*, T. Provder, J. Texter (Eds.), pp. 45–60, ACS Symposium Series (2004).
[310] G. Orts-Gil, K. Natte, D. Drescher, H. Bresch, A. Mantion, J. Kneipp, W. Oesterle. *J. Nanopart. Res.* **13**, 1593 (2011).
[311] W. Anderson, D. Kozak, V. A. Coleman, A. K. Jamting, M. Trau. *J. Colloid Interf. Sci.* **405**, 322 (2013).
[312] J. S. Taurozzi, V. A. Hackley, M. R. Wiesner. *Nanotoxicology* **5**, 711 (2011).
[313] ISO 9277, Determination of the specific surface area of solids by gas adsorption – BET method (2010).
[314] J. Rouquerol, D. Avnir, C. W. Fairbridge, D. H. Everett, J. H. Haynes, N. Pernicone, J. D. F. Ramsay, K. S. W. Sing, K. K. Unger. *Pure Appl. Chem.* **66**, 1739 (1994).
[315] A. Weibel, R. Bouchet, F. Boulc'h, P. Knauth. *Chem. Mater.* **17**, 2378 (2005).
[316] ISO 13099-2, Colloidal systems – Methods for zeta-potential determination – Part 2: Optical methods (2012).
[317] ISO 13099-1, Colloidal systems – Methods for zeta-potential determination – Part 1: Electroacoustic and electrokinetic phenomena (2012).
[318] ASTM E2865-12, Standard Guide for Measurement of Electrophoretic Mobility and Zeta Potential of Nanosized Biological Materials (2012)
[319] A. Hennig, P. M. Dietrich, F. Hemmann, T. Thiele, H. Borcherding, A. Hoffmann, U. Schedler, C. Jäger, U. Resch-Genger, W. E. S. Ungera. *Analyst* **140**, 1804 (2015).